(2)

NAVAL POSTGRADUATE SCHOOL
Monterey, California

THESIS

UNSTEADY FLOW ABOUT POROUS CAMBERED PLATES

by

Paul Jack Lindsey

June 1988

Thesis Advisor: T. Sarpkaya

Approved for public release; distribution is unlimited.

Unclassified

Security Classification of this page AD-A202

REPORT DOCUMENTATION PAGE

1a Report Security Classification: Unclassified	1b Restrictive Markings
2a Security Classification Authority	3 Distribution Availability of Report: Approved for public release; distribution is unlimited.
2b Declassification/Downgrading Schedule	
4 Performing Organization Report Number(s)	5 Monitoring Organization Report Number(s)
6a Name of Performing Organization: Naval Postgraduate School; 6b Office Symbol (*If Applicable*): 69	7a Name of Monitoring Organization: Naval Postgraduate School
6c Address (*city, state, and ZIP code*): Monterey, CA 93943-5000	7b Address (*city, state, and ZIP code*): Monterey, CA 93943-5000
8a Name of Funding/Sponsoring Organization; 8b Office Symbol (*If Applicable*)	9 Procurement Instrument Identification Number
8c Address (*city, state, and ZIP code*)	10 Source of Funding Numbers: Program Element Number; Project No; Task No; Work Unit Accession No
11 Title (*Include Security Classification*): Unsteady Flow About Porous Cambered Plates	
12 Personal Author(s): Paul J. Lindsey	
13a Type of Report: Mechanical Engineer; 13b Time Covered: From To	14 Date of Report (*year, month,day*): June 1988; 15 Page Count: 63
16 Supplementary Notation	
17 Cosati Codes: Field / Group / Subgroup	18 Subject Terms (*continue on reverse if necessary and identify by block number*): Unsteady Flow, Discrete Vortex Analysis, Parachute, Vortex Motion, Porosity

19 Abstract (*continue on reverse if necessary and identify by block number*)

The investigation dealt with the numerical and experimental investigation of the effect of porosity on the vortex shedding from a cambered plate. The effect of porosity was incorporated into the analysis through the use of experimentally obtained pressure-drop data. The results have shown that the porosity of the existing materials used in parachute canopies is not sufficient to eliminate the negative pressure gradient. Canopies with nonuniform porosities will have to be designed to overcome the collapse phenomenon resulting from the unfavorable pressure gradients.

20 Distribution/Availability of Abstract: [X] unclassified/unlimited [ ] same as report [ ] DTIC users	21 Abstract Security Classification: Unclassified
22a Name of Responsible Individual: Professor T. Sarpkaya	22b Telephone (*Include Area code*): (408) 646-3425; 22c Office Symbol: 69-SL

DD FORM 1473, 84 MAR 83 APR edition may be used until exhausted

All other editions are obsolete

security classification of this page: Unclassified

Approved for public release; distribution is unlimited.

Unsteady Flow About Porous Cambered Plates

by

Paul Jack Lindsey
Lieutenant, United States Navy
B.S.M.E., University of California, Berkeley, 1980

Submitted in partial fulfillment of the
requirements for the degree of

MASTER OF SCIENCE IN MECHANICAL ENGINEERING
and
MECHANICAL ENGINEER

from the

NAVAL POSTGRADUATE SCHOOL
June 1988

Author: Paul Jack Lindsey

Approved by: T. Sarpkaya, Thesis Advisor

Anthony J. Healy, Chairman,
Department of Mechanical Engineering

Gordon E. Schacher, Dean of
Science and Engineering

ABSTRACT

The investigation dealt with the numerical and experimental investigation of the effect of porosity on the vortex shedding from a cambered plate. The effect of porosity was incorporated into the analysis through use of the experimentally obtained pressure-drop data. The results have shown that the porosity of the existing materials used in parachute canopies is not sufficient to eliminate the negative pressure gradient. Canopies with *nonuniform porosities* will have to be designed to overcome the collapse phenomenon resulting from the unfavorable pressure gradients.

TABLE OF CONTENTS

LIST OF TABLES

LIST OF FIGURES

TABLE OF SYMBOLS AND ABBREVIATIONS

A Ambient flow acceleration

4b Chord length of the cambered plate

c Radius of the circular cylinder

C_p Pressure coefficient, $C_p = \sqrt{\frac{2\Delta p}{\rho V_N^2}}$

i $\sqrt{-1}$

m Offset of cylinder in the circle plane for transformation

r Radial distance

T Nondimensional time, $T = \frac{Ut}{c}$

U Ambient flow velocity

U_o Reference velocity

V_N Velocity normal to the camber

W Complex potential function

z Nondimensional location in the physical plane

α Porosity coefficient (0.0–1.0)

Δp Differential pressure

Δt Time increment

δ Velocity attenuation factor

Γ_n Circulation of the nth vortex

Γ_o Circulation of the nascent vortex

ρ Density (in slugs/ft^3)

θ Angular coordinate measured counter-clockwise

ζ Nondimensional location in the circle plane

ζ_o Location of the nascent vortex in the circle plane

ACKNOWLEDGMENTS

The author would like to express his sincere gratitude to Distinguished Professor T. Sarpkaya for his guidance, advice, and dedication throughout this research. His enthusiasm and unfailing commitment to the investigation of new and previously unresearched phenomena have been highly motivating.

The author also wishes to thank Mr. Jack McKay of the Mechanical Engineering Department for his skill and workmanship in the construction of the experimental apparatus.

In closing, this research could not have been possible without the love, support, and understanding of his wife Kimberly.

I. INTRODUCTION

The current parachute-canopy design methodology is mainly empirical. It is based on either model tests in wind tunnels (see, e.g., Klimas and Rogers, 1977; Pepper, 1986; Rychnovsky, 1977) or on the deployment of full-scale parachutes with test loads. However, under certain conditions, parachutes have been observed to collapse during periods of rapid deceleration, subsequent to the initial inflation of the canopy with a resulting loss of drag and ultimately the payload.

Studies began with a two-dimensional model of flow about a rigid, nonporous camber. Even though highly idealized, the purpose of the investigation was not a solution of an immediate practical problem but to understand the physics of the problem. With that in mind, the discrete vortex model (DVM) (see, e.g., Chorin, 1973; Sarpkaya, 1975) was used to model the flow past bodies with included angles of 120, 180, and 240 degrees, and was analyzed by Mostafa (1987) and Munz (1987). These investigations have shown that the drag force is predicted fairly well during the steady-state period and up to the middle of the deceleration period. Beyond that time, the predicted forces tended to be relatively larger than those measured experimentally.

Nevertheless, the forces measured during the final stages of deceleration were very small, so the degree of exactness was not a concern. Moreover, the reasons leading to the collapse (backwash of the vortices) occurred shortly after the start of deceleration, where

the predicted and measured forces compared well. Previous investigations at the Naval Postgraduate School have concluded that the development of negative differential pressures in the central region of the camber is the likely cause of parachute collapse at high deceleration rates (see, e.g., Munz, 1987).

In view of the foregoing, it became clear that the flow through the porous camber, if managed properly, can help to minimize or eliminate the collapse phenomenon by eliminating the negative differential pressure across certain sections of the camber. The present investigation was undertaken to study in detail the effect of porosity on a two-dimensional rigid camber in order to bring the theoretical problem a step closer to reality. In the following, the fundamental concepts used in the introduction of flow through a porous wall and the results obtained with various methods and porosities are described in detail.

II. EFFECTS OF POROSITY

A. REVIEW OF THE FLOW THROUGH POROUS SCREENS

A parachute canopy is a porous material. The amount of flow that goes through such a material depends on the percentage area opening, the shape and size of the threads, the moisture content of the material, the differential pressure across the canopy, the angle of approach of the ambient flow, the magnitude and direction of the flow on the downstream side of the canopy, and the degree of time-dependence of the upstream and downstream flows (i.e., the vortex motion downstream of a parachute).

In order to incorporate the effect of porosity into the analysis, one had to know at least the flow rate through the canopy as a function of differential pressure, assuming that all of the other parameters cited above were of secondary importance, or that their effects may be incorporated into a flow coefficient relating differential pressure to the normal velocity of the flow rate. This seemingly simple search for a reliable (theoretical and/or experimental) equation turned out to be anything but simple. The following is a brief description of the previous investigations of the flow past screens.

A fairly detailed review of the flow through screens is given by Laws and Livesy (1978). There are a number of investigations (see, e.g., Baines and Peterson, 1951; Turner, 1969; Reynolds, 1969; Graham, 1976) which dealt with the flow past fairly porous screens for

the purpose of understanding, managing, or generating isotropic turbulence. Often the resistance through the screen was of minor importance. Others (see e.g., Taylor, 1944; Taylor and Davies, 1944; Wieghardt, 1953) who investigated the flow through infinite screens expressed the resistance as

$$\Delta p = \tfrac{1}{2}\rho K U^2$$

Koo and James (1973) and Cumberbatch (1982) investigated the flow past finite screens set in infinite flows, but the effects of body shape, separation, vortex formation, flow magnitude and direction downstream of the body, and deceleration of the flow were not studied. It became clear that there was an enormous amount of research done on the flow through screens and yet there was very little information which could be extracted from them for use in this study of a decelerating parachute. Payne (1978) reviewed the data from many researchers in an effort to relate the geometric porosity (open area ratio) to the differential pressure, and developed an equation in terms of dynamic pressure loss term and a viscous loss term,

$$\Delta p = K_1 U^2 + K_2 U$$

However, this study involved many different cloth types, not just parachute cloth, and included no evaluations of the effects of flow direction. This prompted the undertaking of an experimental investigation to establish the proper relationship between the pressure drop,

the flow rate, and the flow direction on the actual samples of canopy materials used in parachutes.

B. PARACHUTE CLOTH EXPERIMENTS

1. Experimental Apparatus and Procedure

The purpose of the experiments was twofold: to find the differential pressure versus flow rate relationship, and to find the change, if any, of this relationship with the downstream flow direction. For this purpose, an experimental apparatus was conceived, designed, and manufactured as shown in Figures 1 and 2. The flow rates at points A and B were measured with the standard flow meters, and the static pressures upstream of the screen were recorded for each flow rate through the screen. Static pressure downstream of the screen was assumed to be atmospheric.

Observations have shown that the canopy sample did not bulge measurably during the experiments, even at the differential pressures encountered by a parachute beginning to descend at a speed of about 600 miles per hour. This was primarily due to the proper construction and sandwiching of the circumference of the canopy sample. However, this is not meant to exclude the possibility that at high pressures, the slight cambering of the sample may have stretched it and thereby increased its porosity slightly, leading to a smaller differential pressure for a given flow rate than that had it not been stretched. In fact, this was checked by conducting the experiments first with increasing flow rate and then decreasing the flow rate. No

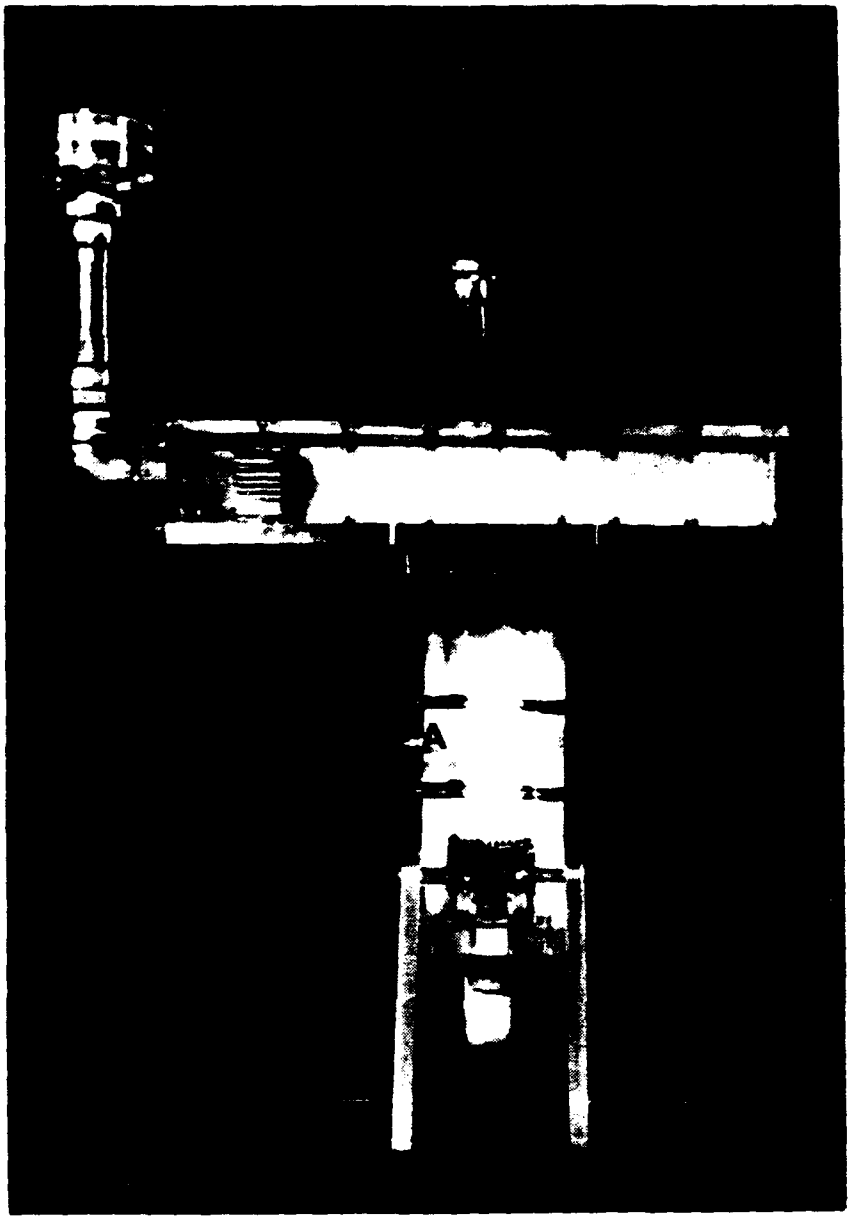

Figure 1. **Parachute Cloth Differential Pressure Measurement Apparatus, Front View**

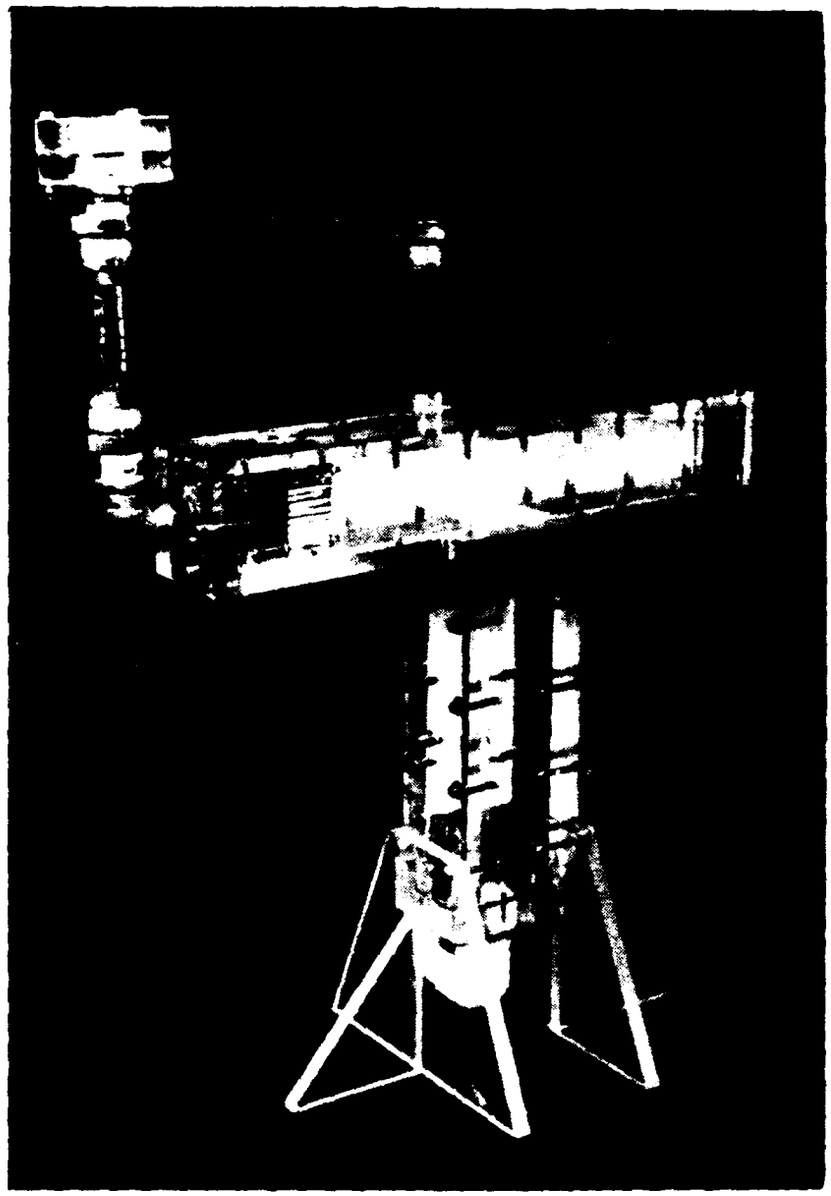

Figure 2. **Parachute Cloth Differential Pressure Measurement Apparatus, Three-Quarters View**

attempt was made to wait a long time after the completion of the experiment with ascending pressures to see if the material would return to its original unstretched shape, or whether fibers used in construction of the canopies develop a permanent set beyond certain differential pressures and retain their deformed shape. This leads to the possibility that a once-used parachute may fall faster than a never-used one.

Of the seven available canopy materials, four samples were chosen and tested to provide a range of data. The characteristics of the four samples are shown in Table 1. The identifying letters are used for later reference.

TABLE 1

CHARACTERISTICS OF PARACHUTE CLOTH SAMPLES

Sample Letter	Material	Weight	Military Specifications Number
A	Nylon	1.1 oz.	–
B	Nylon	4.75 oz.	MIL-C-8021D Type I
C	Nylon	7.0 oz.	MIL-C-8021D Type II
D	Kevlar	3.0 oz.	–

During the course of the experiments, the flow on the down-stream face of the sample was systematically changed to see if the

differential pressure across the sample would increase for a given flow rate through the sample.

2. Results

The results of tests on the effect of flow on the downstream face of the samples have emphatically and somewhat surprisingly shown that the flow through the screens investigated is not affected by the presence or absence of the downstream flow. This apparently simple finding is of extreme mathematical and practical importance. It simplifies the analysis and the possible management of porosity to eliminate parachute collapse.

The results obtained with the four representative canopy samples are shown in Figures 3 and 4.

Figure 3 shows the variation of differential pressure as a function of the dynamic head, $\frac{1}{2}\rho V_N^2$, where V_N is the velocity through the canopy $\left(\frac{Q}{A}\right)$. It is clear that the value of differential pressure varies with the weight of the sample and manufacturing. For samples B and C, the military specifications expressed the mean velocity as flow rate per unit area. For both samples, the military specifications call for 50 to 90 cfm/ft^2 at a differential pressure of .5 inch of water, and 450 to 650 cfm/ft^2 at a differential pressure of 20 inches of water. Sample B extrapolated to 88 cfm/ft^2 and 654 cfm/ft^2, respectively, and sample C extrapolated to 89 cfm/ft^2 and 487 cfm/ft^2, respectively.

Figure 4 shows the pressure coefficient C_p, defined by

$$C_p = \sqrt{\frac{2\Delta p}{\rho V_N^2}}$$

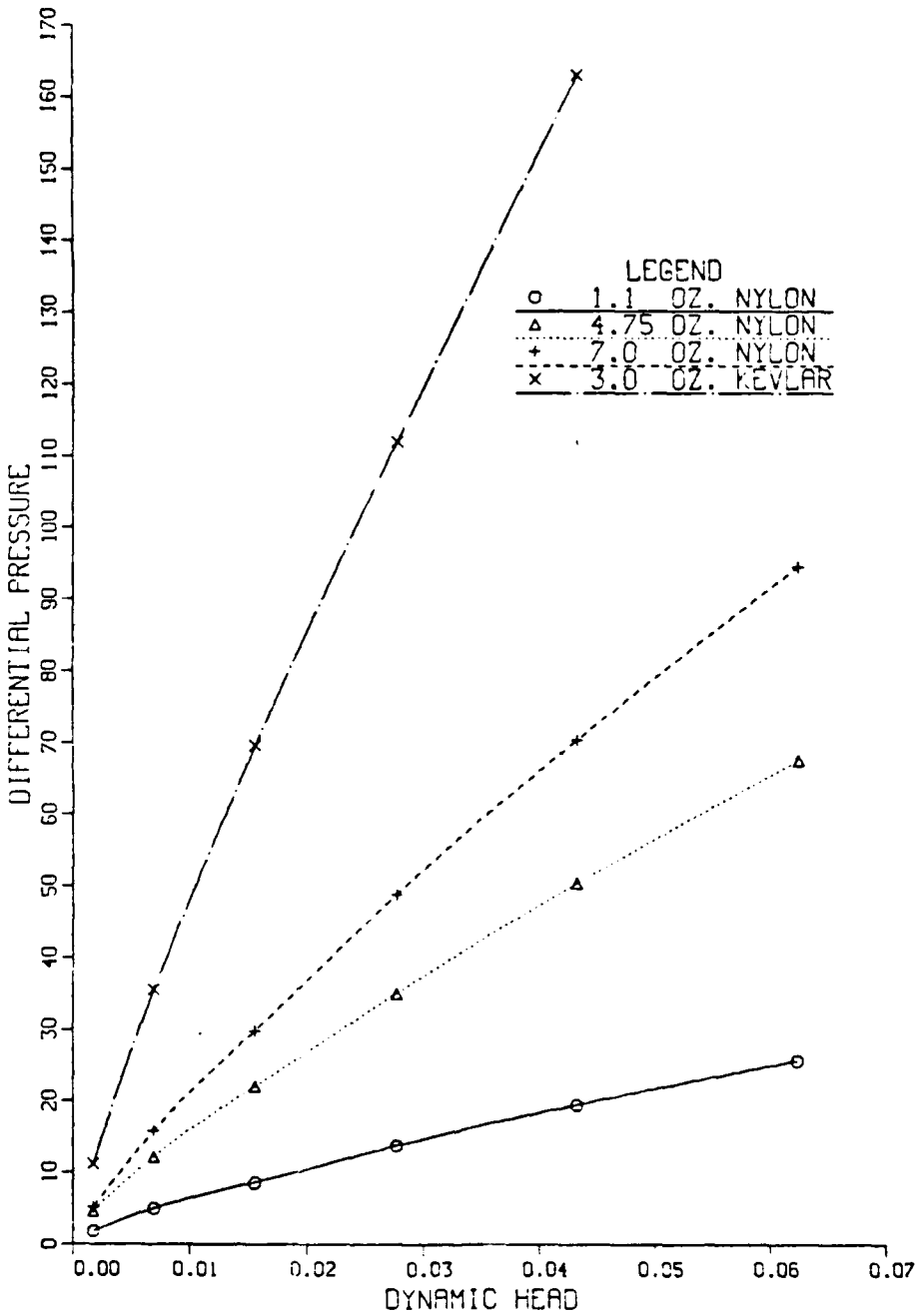

Figure 3. **Differential Pressure vs. Dynamic Head for Parachute Cloth Samples**

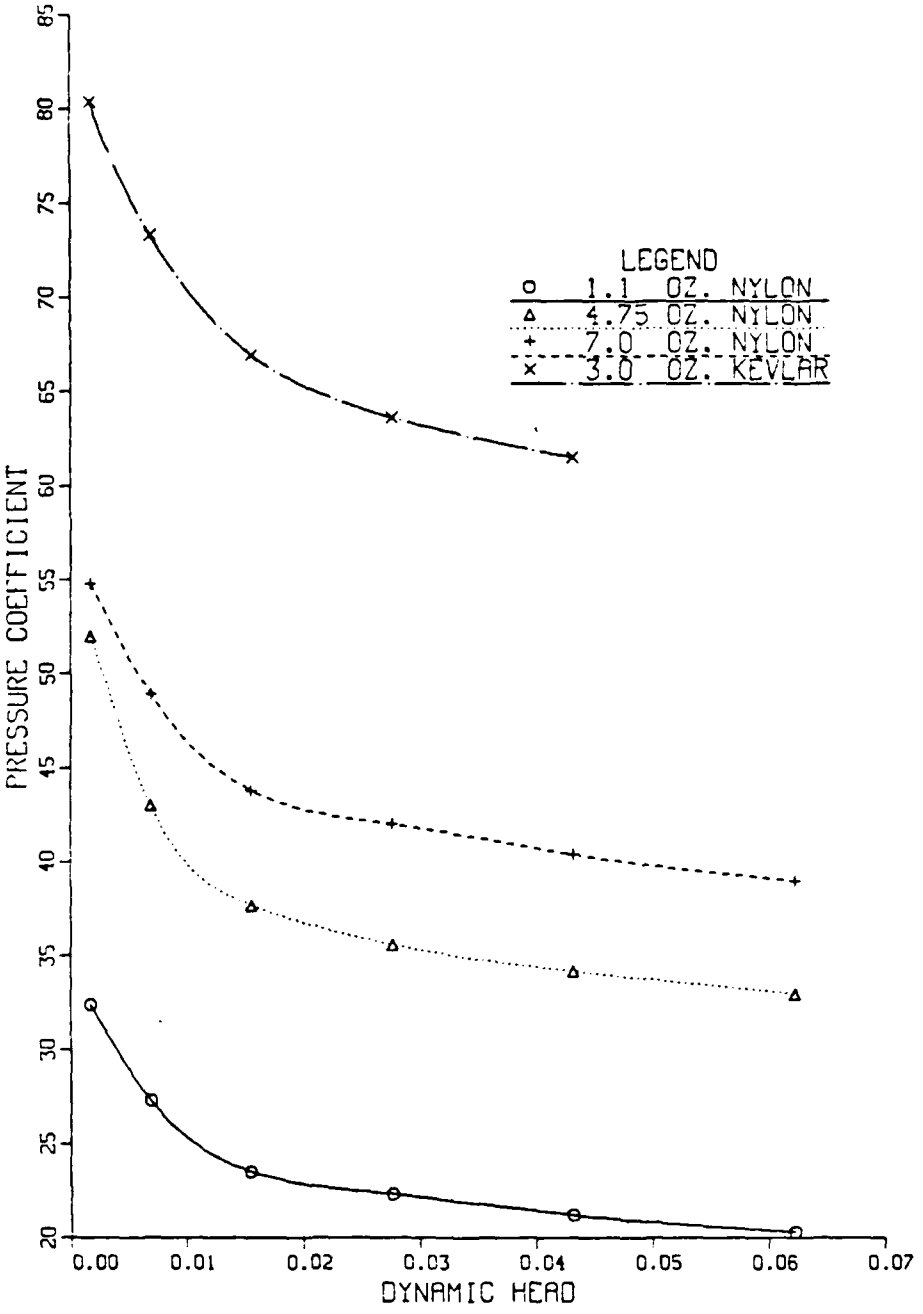

Figure 4. **Pressure Coefficient vs. Dynamic Head for Parachute Cloth Samples**

for all the samples as a function of dynamic head. Clearly, the pressure coefficient remains nearly independent of velocity for a given canopy. As noted earlier, the flow on the downstream face of the sample (which ranged from 0 to 14.4 ft/sec) had no effect on the results shown in Figures 3 and 4. Table 2 shows the minimum, maximum, and average values of the pressure coefficient for the different samples.

TABLE 2

COMPARISON OF THE PRESSURE COEFFICIENTS FOR THE DIFFERENT CANOPY MATERIAL SAMPLES

Sample	Minimum C_p	Maximum C_p	Average C_p
A	20.3	27.3 (32.4)	22.9 (24.5)
B	33.0	43.0 (52.0)	36.7 (39.2)
C	39.0	48.9 (54.8)	42.8 (44.8)
D	61.5	73.3 (80.4)	66.3 (69.1)

Notes:

(1) The values in parentheses in the maximum column are for the lowest velocity data points.

(2) The average values do not include the pressure coefficients for the lowest velocity data points because they were deemed not representative of the velocities that parachutes descend. The values in parentheses in the average column are averages if these data points had been included.

III. NUMERICAL EXPERIMENTS

A. THEORETICAL FOUNDATIONS OF THE MODEL

The flow about a cambered plate is obtained by successive transformations from a circle plane. In fact, it can be shown that the flow in the ζ-plane (circle plane) may be transformed to the flow in the z-plane (camber plane) through the use of

$$z = \zeta + m - \frac{b^2}{\zeta + m} - \frac{2m^2 - 1}{m}$$

in which m is a parameter related to the total angle of the circular arc. For example, m equal to .5, .707, or .866 corresponds to camber angles of 120, 180, or 240 degrees, respectively. Figure 5 shows the transformation from a circle to a 120-degree camber.

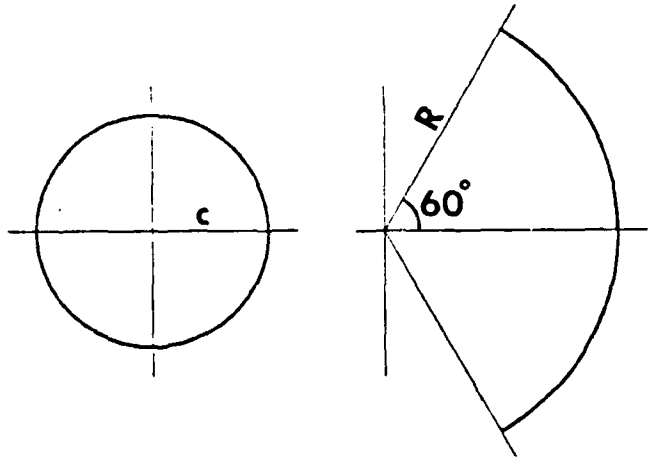

Figure 5. **Circle and Physical Planes**

The complex function describing the flow is given by

$$W = -U\left(\zeta + \frac{c^2}{\zeta}\right) + \frac{i\Gamma_{0p}}{2\pi}\mathrm{Ln}(\zeta - \zeta_{0p}) - \frac{i\Gamma_{0p}}{2\pi}\mathrm{Ln}\left(\zeta - \frac{c^2}{\overline{\zeta}_{0p}}\right)$$
$$+ \sum_{k=1}^{m}\frac{i\Gamma_{kp}}{2\pi}\mathrm{Ln}(\zeta - \zeta_{kp}) - \sum_{k=1}^{m}\frac{i\Gamma_{kp}}{2\pi}\mathrm{Ln}\left(\zeta - \frac{c^2}{\overline{\zeta}_{kp}}\right) - \frac{i\Gamma_{0q}}{2\pi}\mathrm{Ln}(\zeta - \zeta_{0q})$$
$$+ \frac{i\Gamma_{0q}}{2\pi}\mathrm{Ln}\left(\zeta - \frac{c^2}{\overline{\zeta}_{0q}}\right) - \sum_{k=1}^{m}\frac{i\Gamma_{kq}}{2\pi}\mathrm{Ln}(\zeta - \zeta_{kq}) + \sum_{k=1}^{m}\frac{i\Gamma_{kq}}{2\pi}\mathrm{Ln}\left(\zeta - \frac{c^2}{\overline{\zeta}_{kq}}\right)$$

in which Γ_{kp} and ζ_{kp} represent respectively the strength and location of the k-th p-vortex (counter-clockwise rotating), and Γ_{kq} and ζ_{kq} represent the strength and location of the k-th q-vortex (clockwise rotating). As described in Munz, discrete vortices are introduced at the tips of the camber at regular time intervals, and evolution of the vortex wake is calculated through the use of the velocities induced at each vortex location. Furthermore, the forces acting on the camber are calculated through the use of the generalized Blasius theorem, or through the integration of the differential pressure. The numerical model requires the input of a velocity history, and in the present investigation, the velocity profile that was employed was that used by Munz for the simple purpose of delineating the effect of porosity relative to the non-porous case calculated by Munz.

The existing analysis had to be considerably modified in order to incorporate the effect of porosity. The inclusion of the effect of porosity was already shown to be difficult as far as the previous experimental investigations are concerned. It turns out that its mathematical analysis is just as difficult as its experimental understanding.

B. INOUE'S METHOD

The only work which dealt with a *steady uniform* flow past a simple porous flat plate was carried out by Inoue. To emphasize, the flow was not subjected to any deceleration and the only unsteadiness introduced into the flow came from the evolution of the vortex shedding following the impulsive start of the flow at a constant velocity. Inoue made no attempt to relate the differential pressure across the plate to the flow rate. According to his method, the complex function for a plate normal to the flow is given by

$$f_1 = \frac{\alpha\left(\zeta - \frac{1}{\zeta}\right)}{2} + \frac{(1-\alpha)\left(\zeta + \frac{1}{\zeta}\right)}{2} + i\sum_{K=1}^{N}\frac{\Gamma_K}{2\pi}\ln\frac{\zeta-\zeta_K}{\zeta-\overline{\zeta}_K} + i\sum_{L=1}^{N}\frac{\Gamma_L}{2\pi}\ln\frac{\zeta-\zeta_L}{\zeta-\overline{\zeta}_L}$$

in which α is an artificial porosity coefficient related to the geometric porosity and αU_{inf} is the part of the flow which passes through the plate uniformly, regardless of the differential pressure distribution prevailing along the plate. Inoue did not calculate forces or pressure distributions, and confined himself to the comparison of the calculated flow kinematics with sample flow pictures, presumably obtained under conditions similar to those encountered in the numerical calculations.

Inoue's analysis, though not applicable to the analysis of the actual flow under consideration, was tried anyway, to gain some experience regarding the overall performance of the code developed in the present investigation. Figures 6 through 10 show, at representative times, the evolution of flow for α = 0.25 and for the velocity profile given by

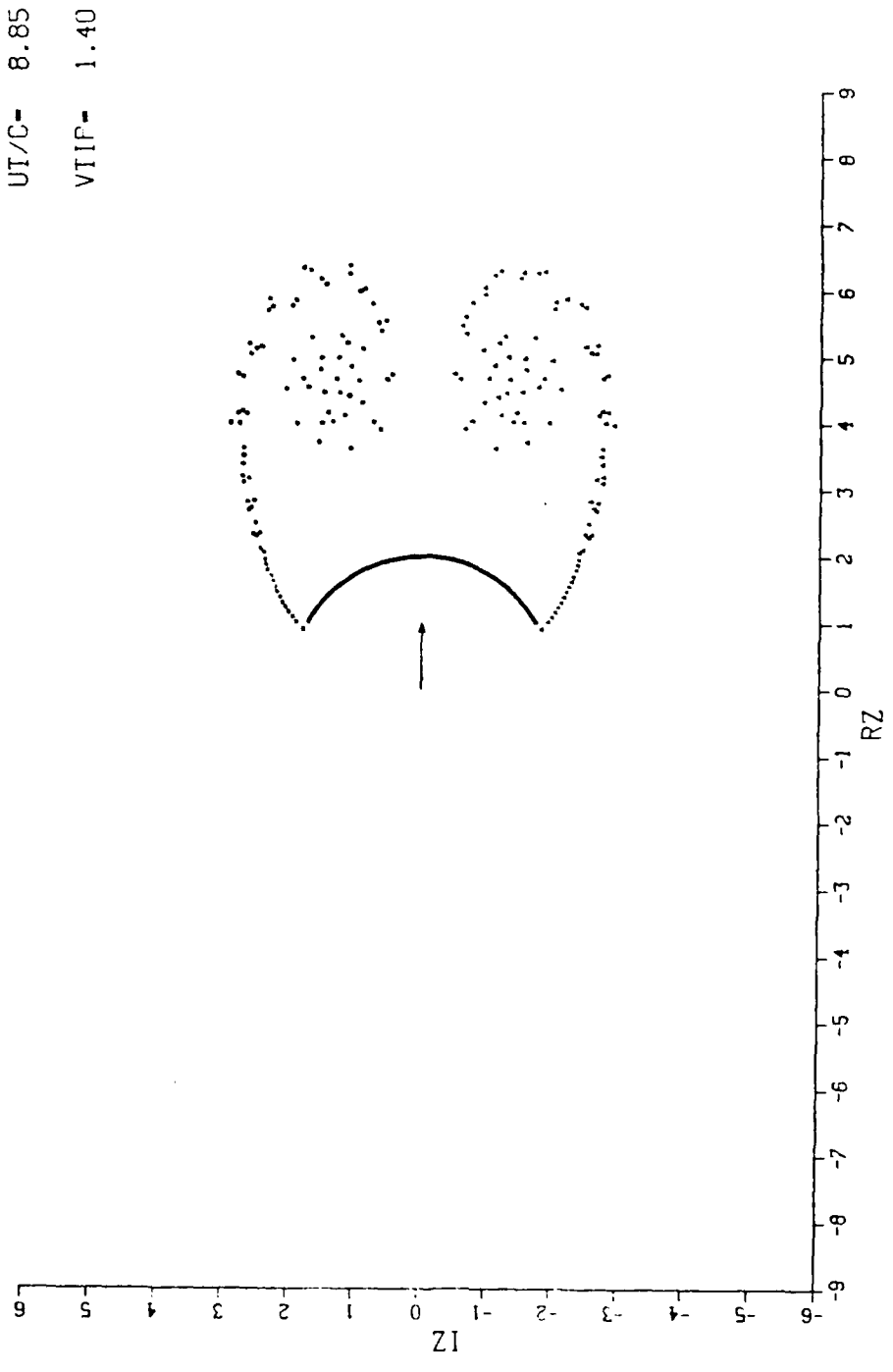

Figure 6. **Wake Vortex Positions for α = 0.25 at T = 8.85**

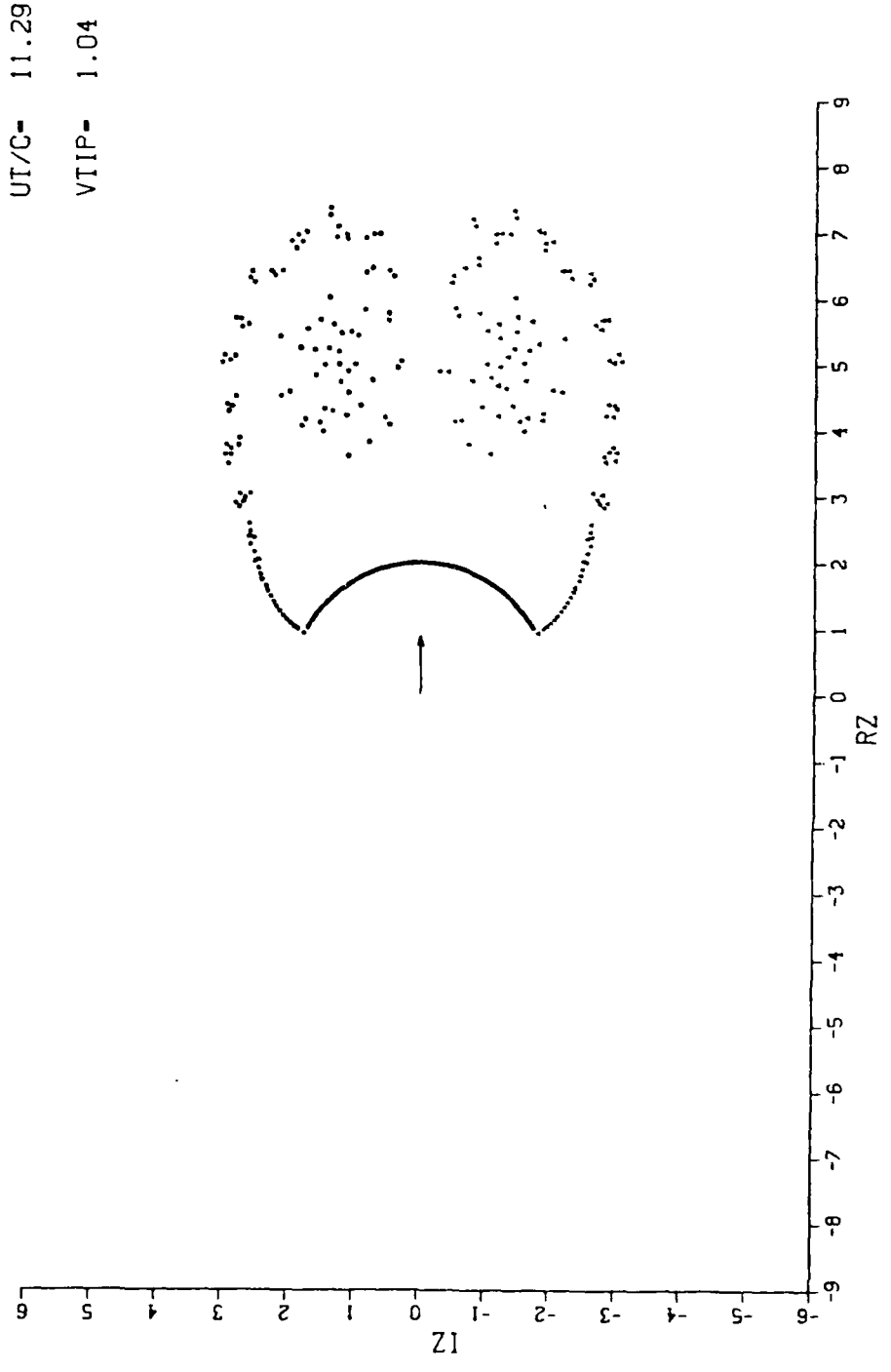

Figure 7. **Wake Vortex Positions for α = 0.25 at T = 11.29**

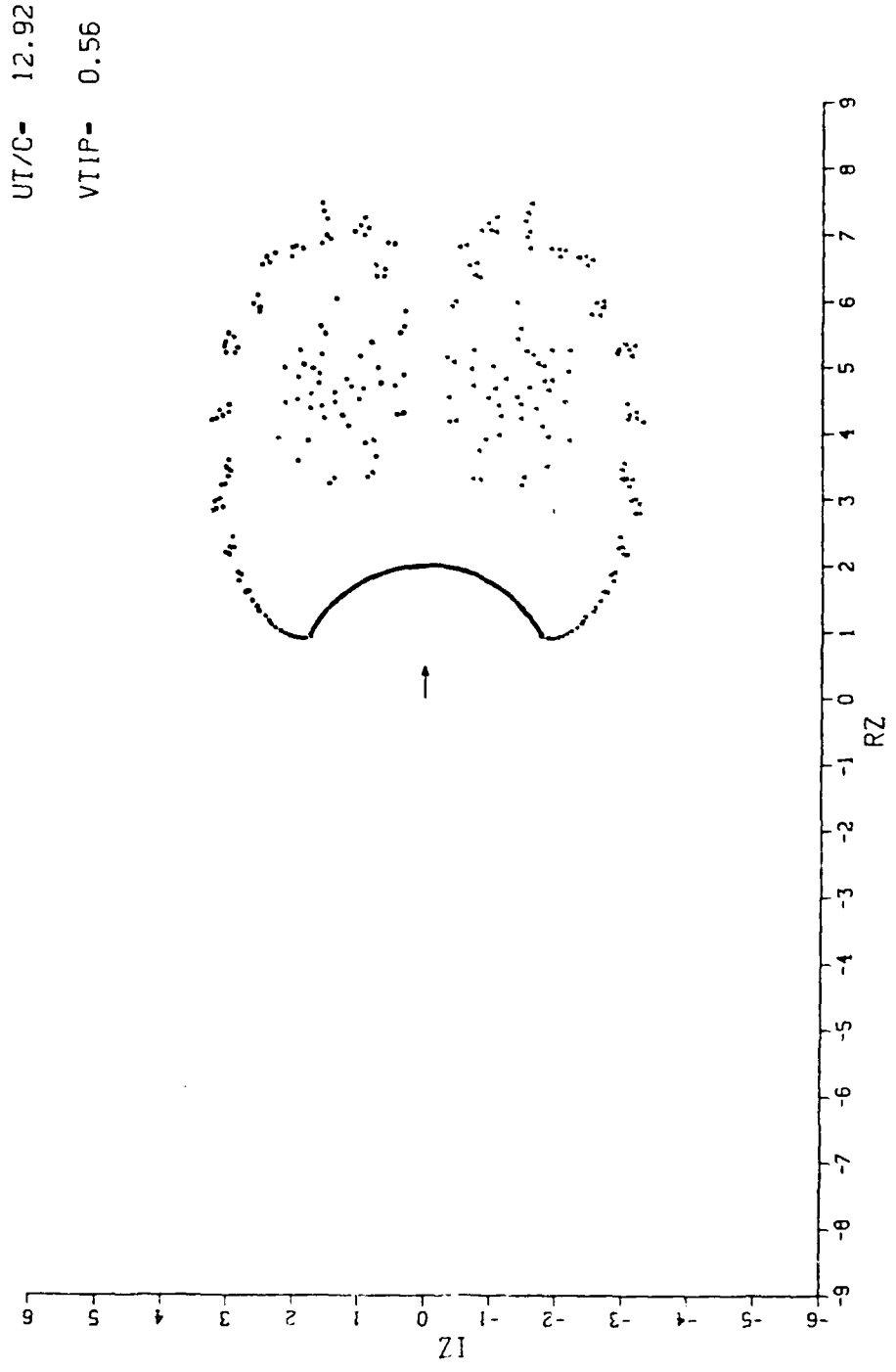

Figure 8. **Wake Vortex Positions for α = 0.25 at T = 12.92**

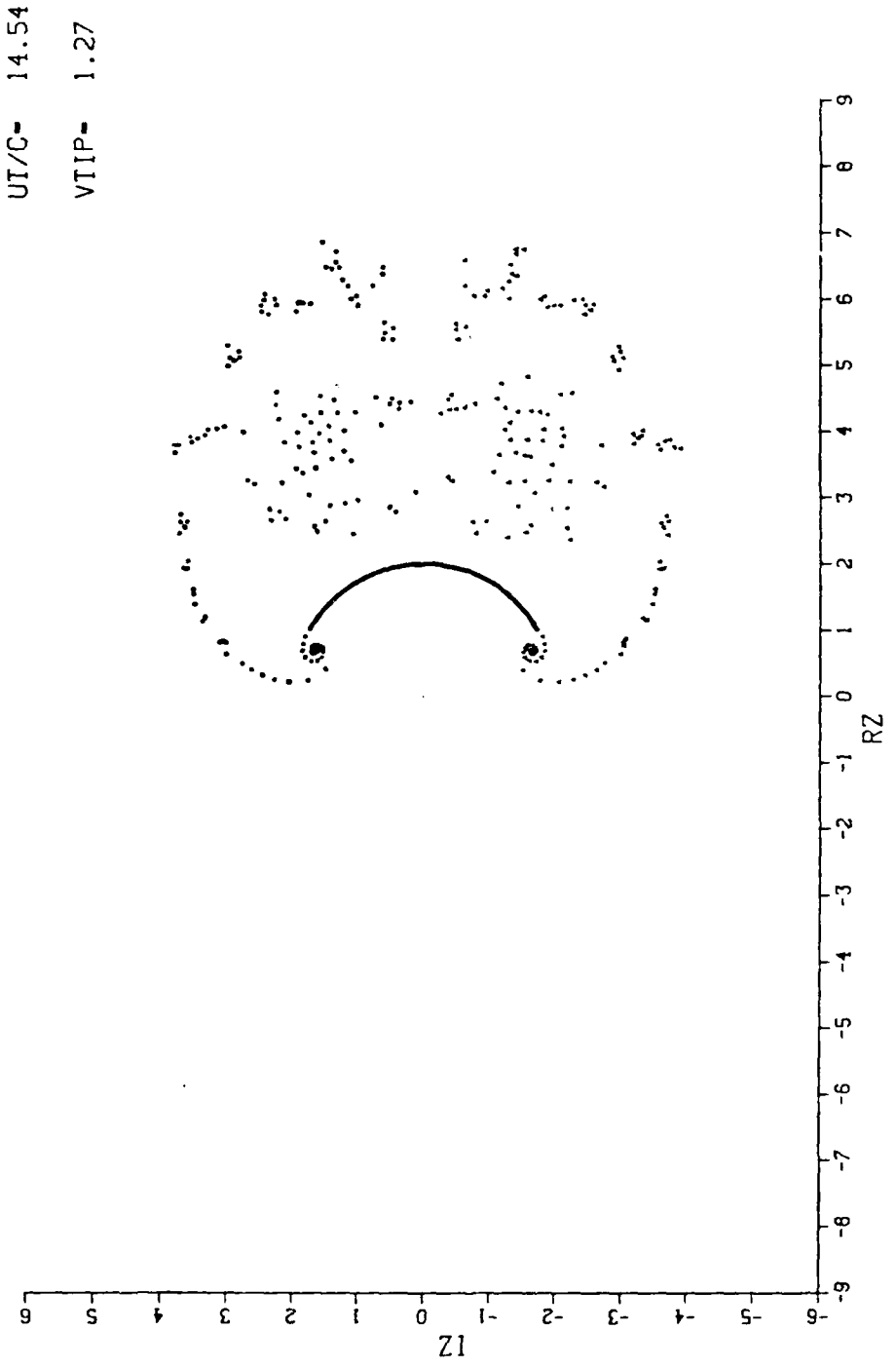

Figure 9. **Wake Vortex Positions for α = 0.25 at T = 14.54**

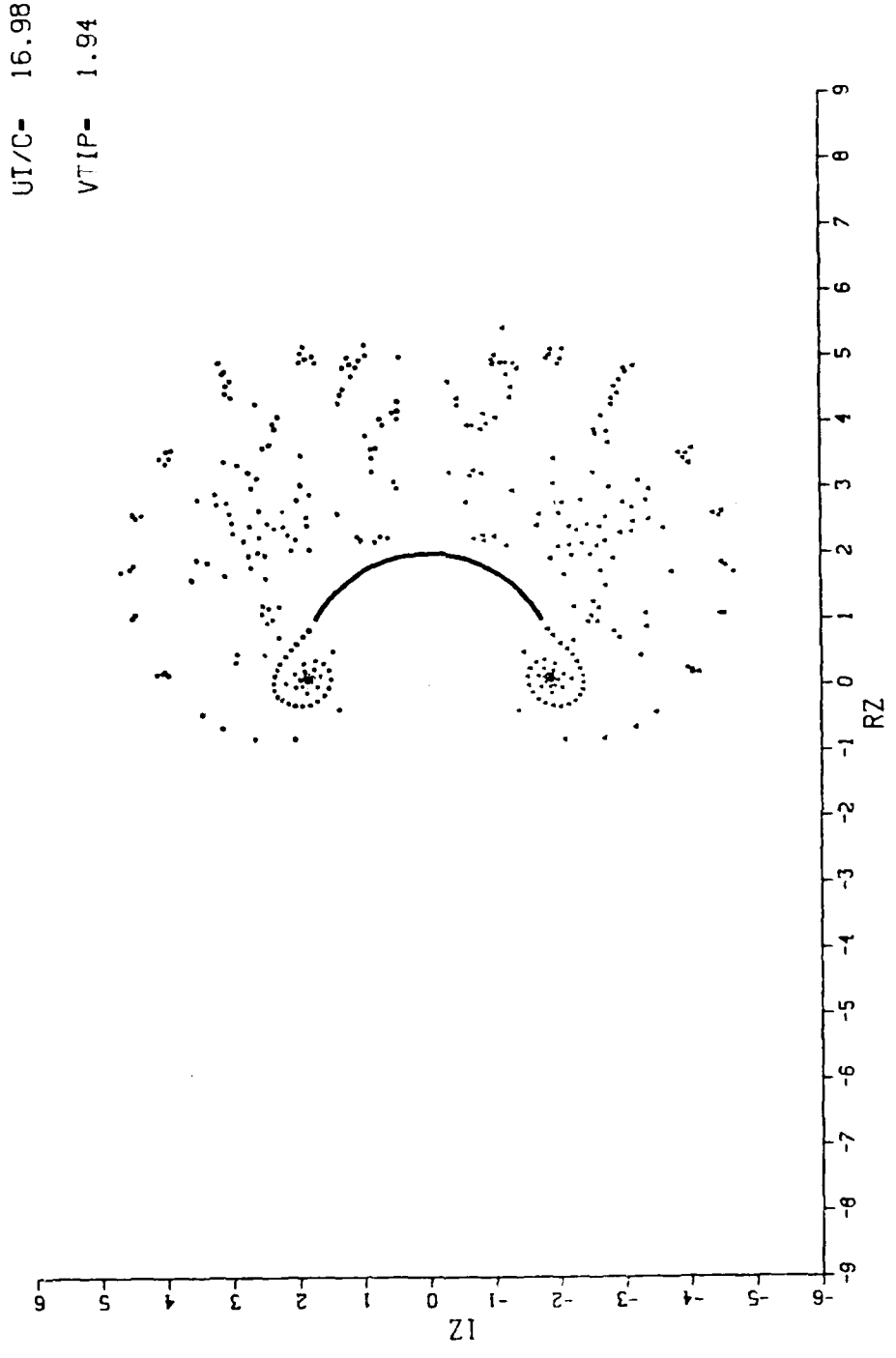

Figure 10. **Wake Vortex Positions for α = 0.25 at T = 16.98**

$$U/U_o = 1 \text{ for } T = U_o t/c \leq 9.72$$

and

$$U/U_o = 0.97T - 0.05T^2 - 3.70$$

and

$$A = 0.97 - 0.10T$$

in the interval $9.72 \leq T \leq 11.48$ and

$$U/U_o = -0.3423 + 0.0072T^2 + 3.82$$

and

$$A = -0.3423 + 0.01445T$$

in the interval $11.48 \leq T \leq 17.95$.

For T greater than 18, the velocity and acceleration are zero.

Figures 11 through 15 show the flow at exactly the same times about a nonporous camber ($\alpha = 0$). Comparison of these figures shows that, as anticipated,the effect of the porosity is to push the wake further downstream and thereby minimize the consequences of the return of the wake to the body. In fact, Figures 16 through 20 show the comparison of the differential pressures at the corresponding times for $\alpha = 0.0$ and 0.25. Apparently, the differential pressure for $\alpha = .25$ becomes less negative than the one for $\alpha = 0.0$, even though, as

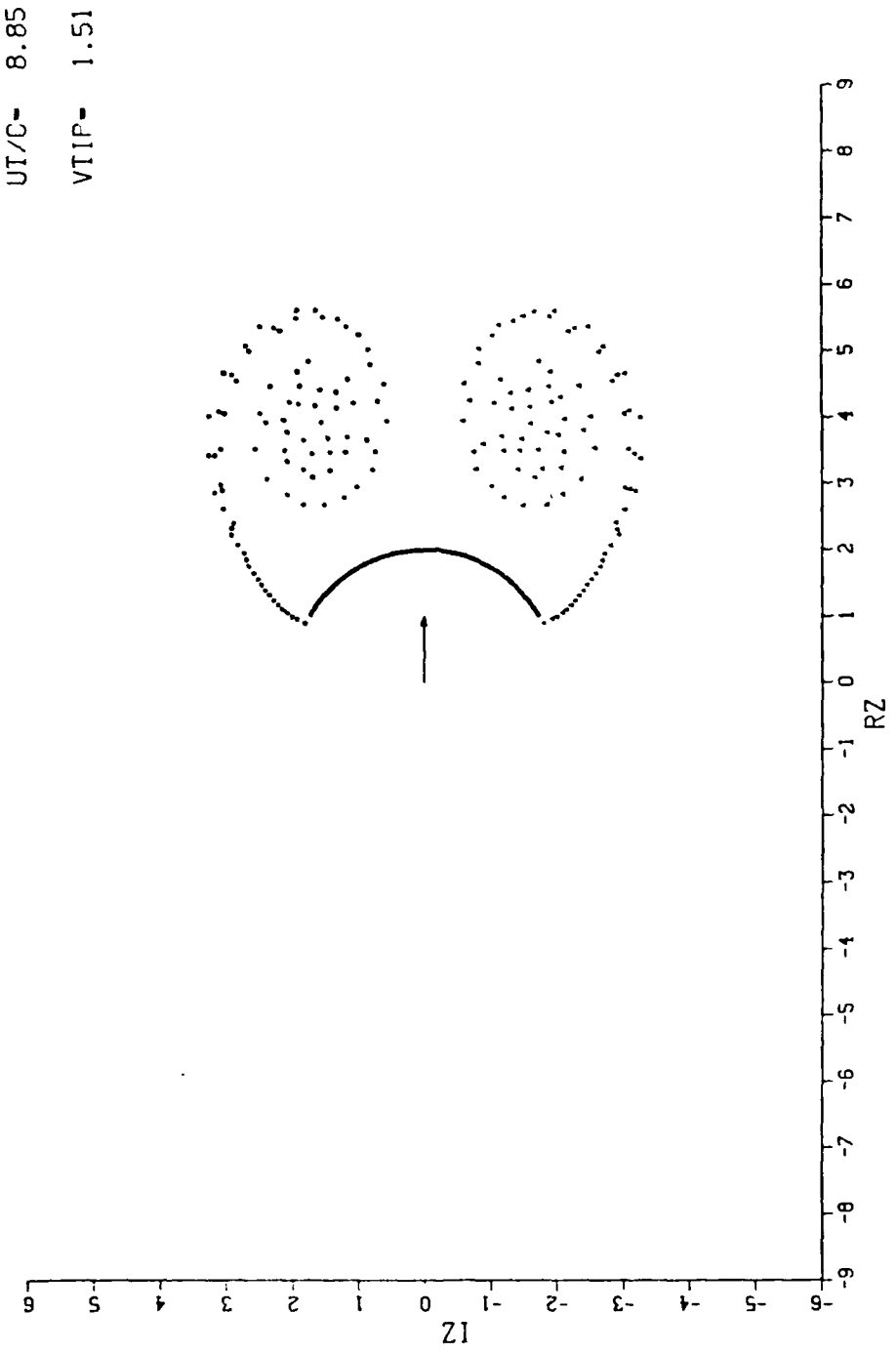

Figure 11. **Wake Vortex Positions for Non-Porous Camber at T = 8.85**

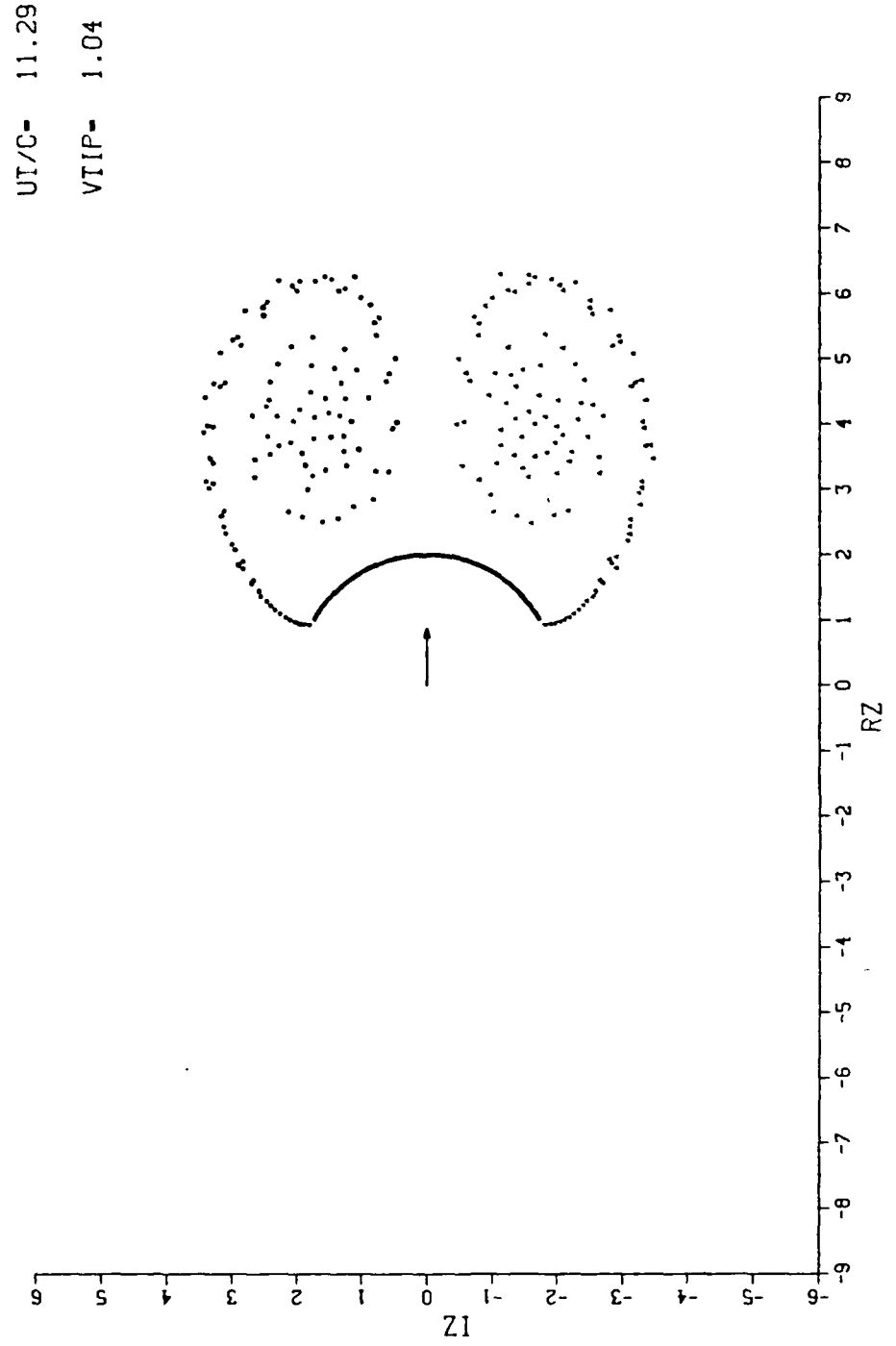

Figure 12. **Wake Vortex Positions for Non-Porous Camber at T = 11.29**

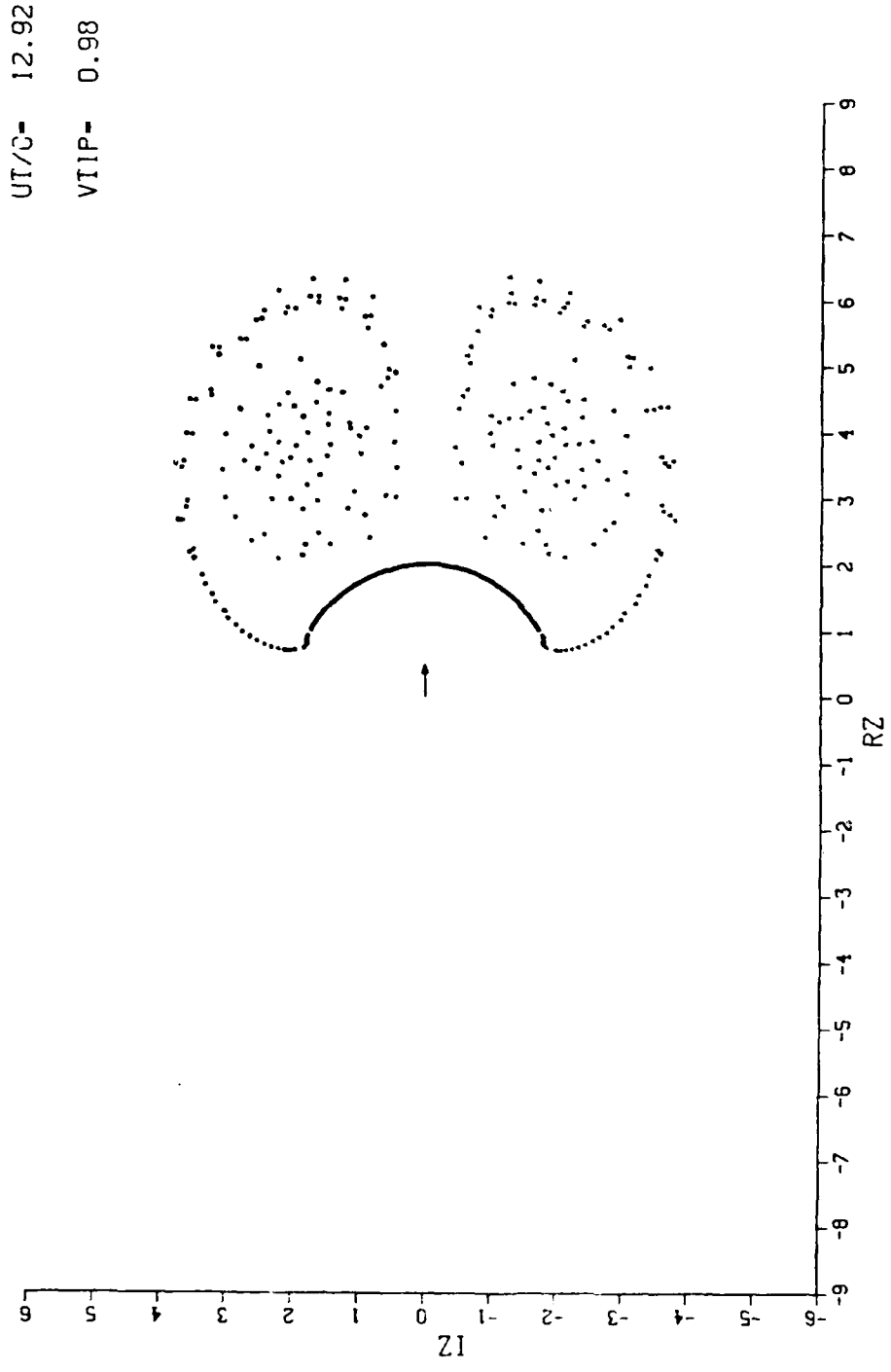

Figure 13. **Wake Vortex Positions for Non-Porous Camber at T = 12.92**

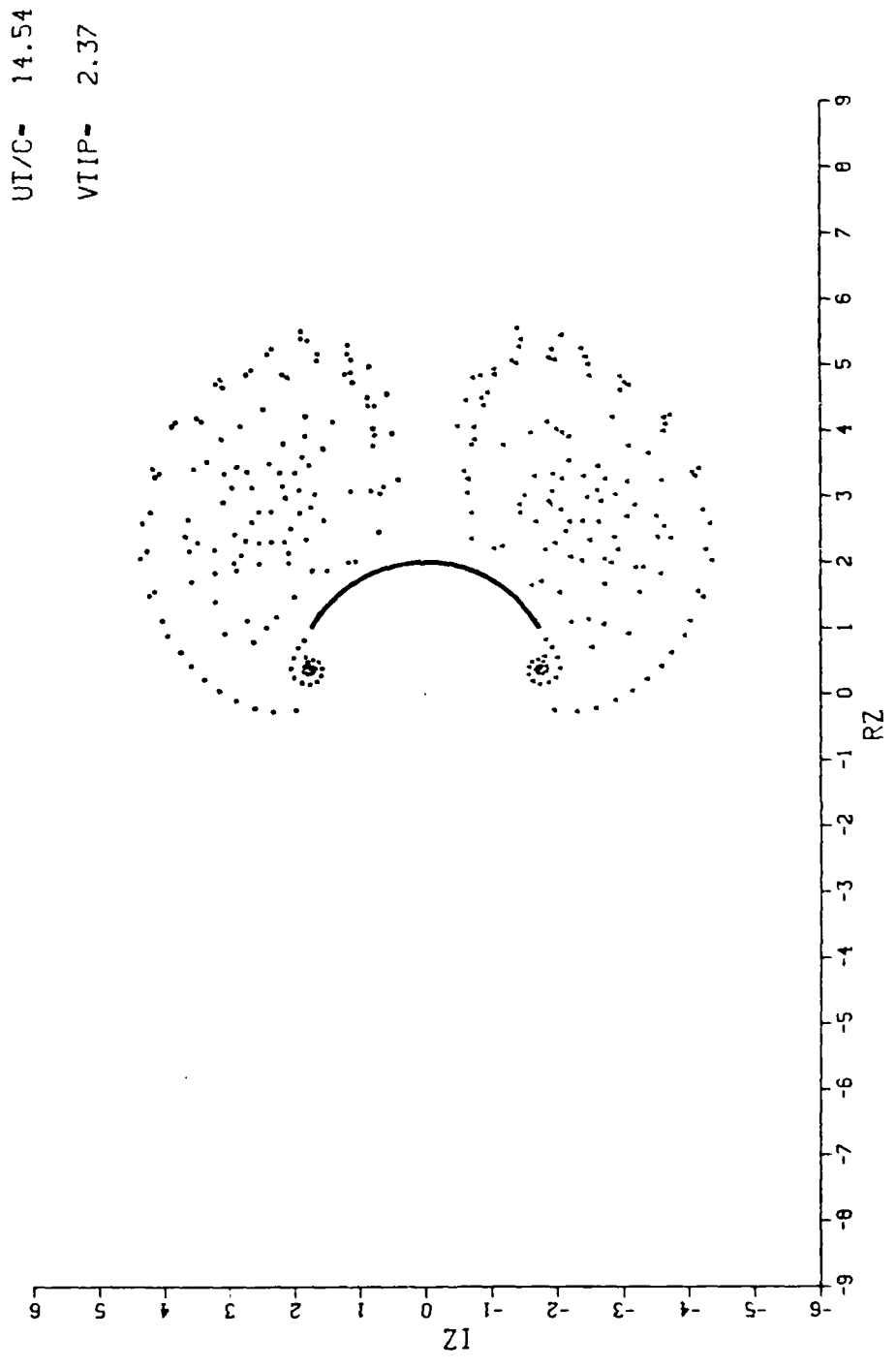

Figure 14. **Wake Vortex Positions for Non-Porous Camber at T = 14.54**

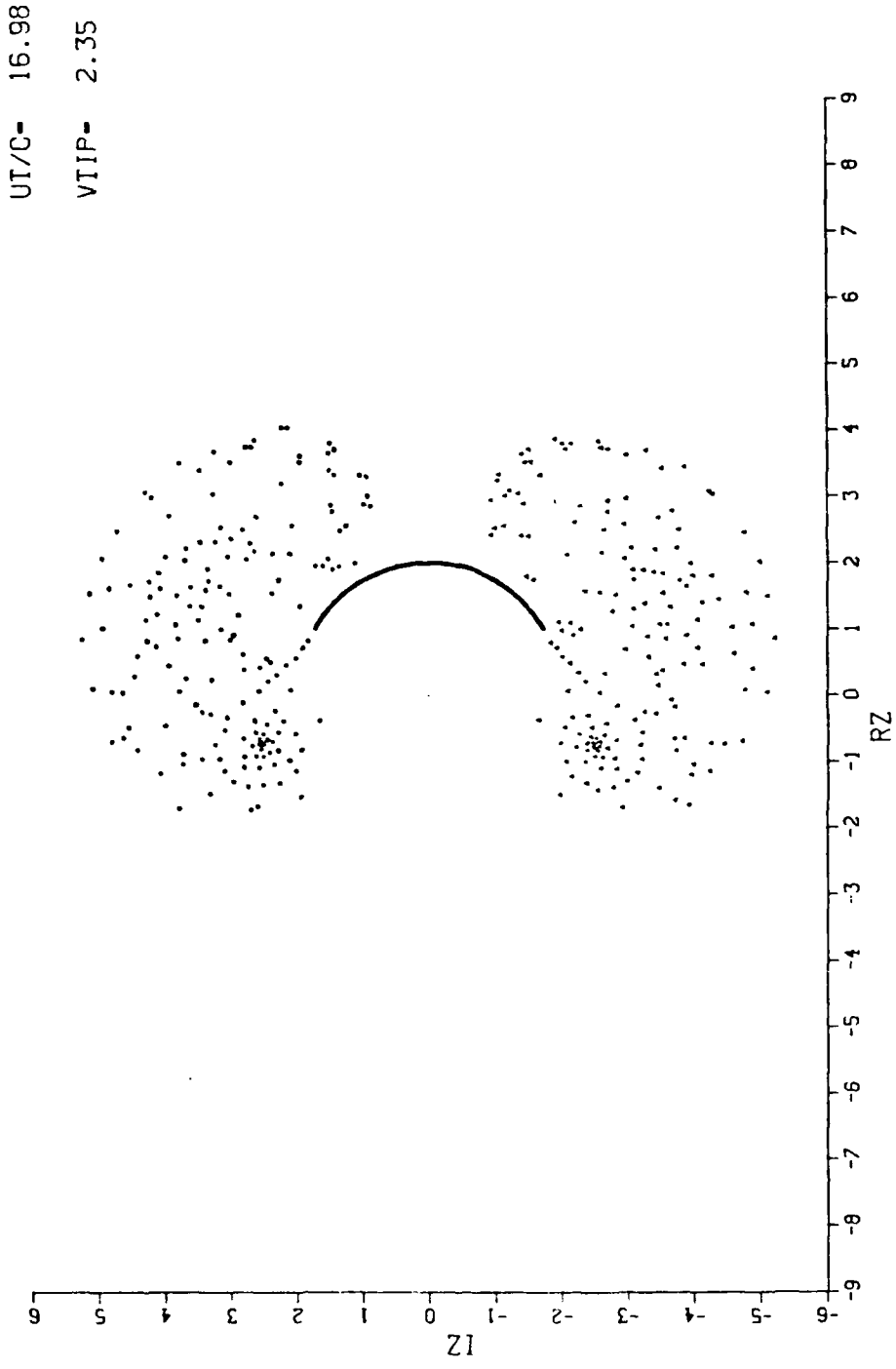

Figure 15. **Wake Vortex Positions for Non-Porous Camber at T = 16.98**

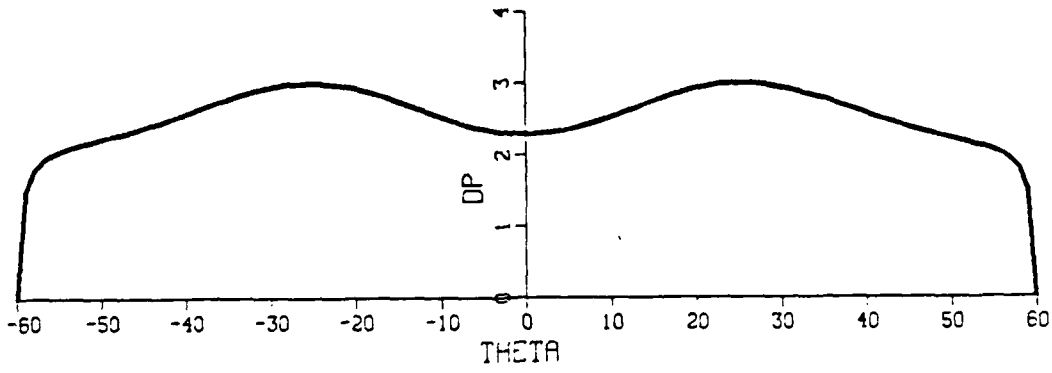

Nonporous Camber

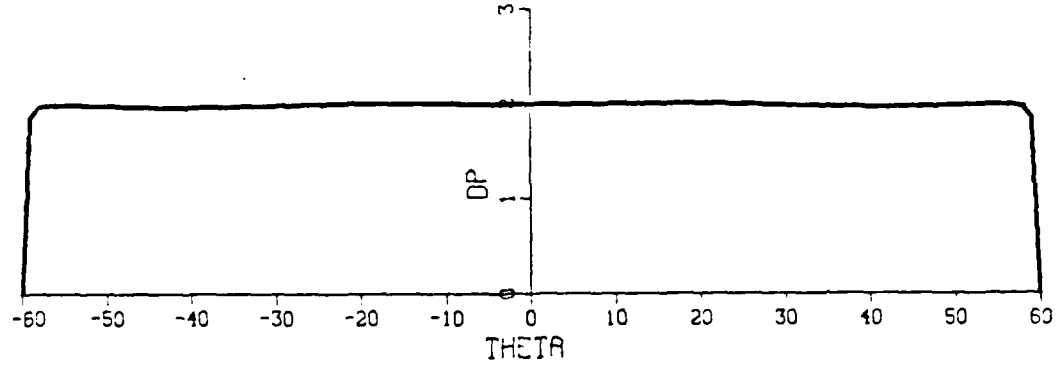

Porous Camber, $\alpha = 0.25$

Figure 16. **Differential Pressure Comparison at T = 8.85**

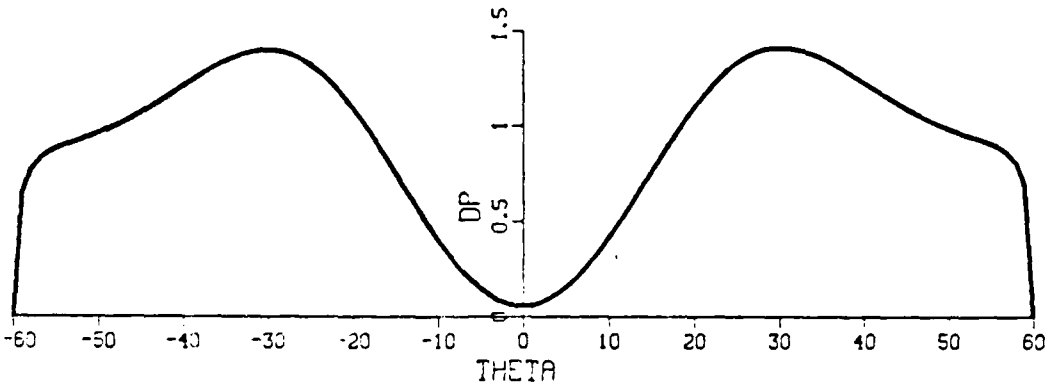

Nonporous Camber

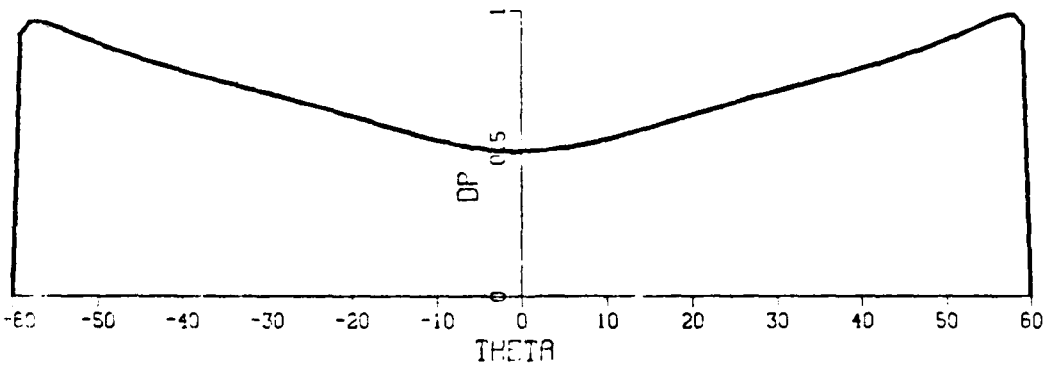

Porous Camber, $\alpha = 0.25$

Figure 17. **Differential Pressure Comparison at T = 11.29**

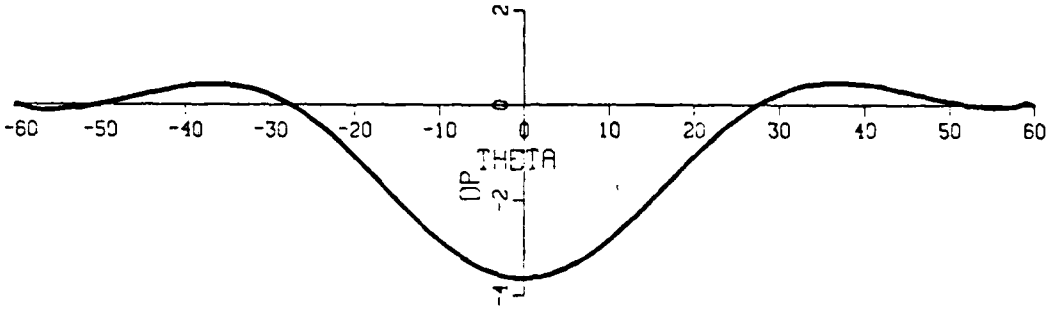

Nonporous Camber

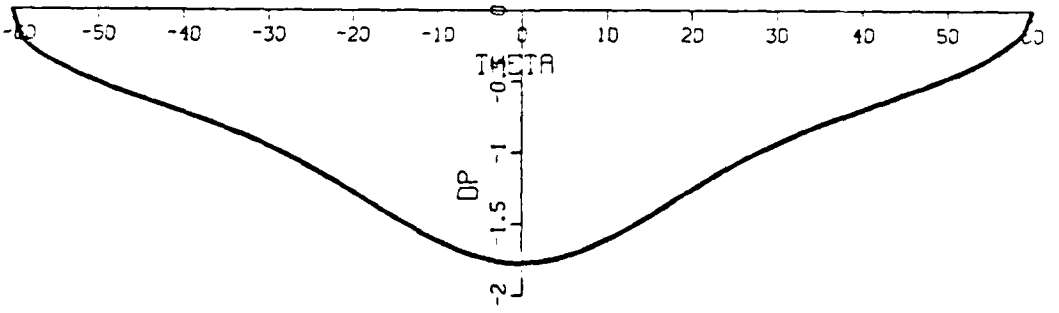

Porous Camber, $\alpha = 0.25$

Figure 18. **Differential Pressure Comparison at T = 12.92**

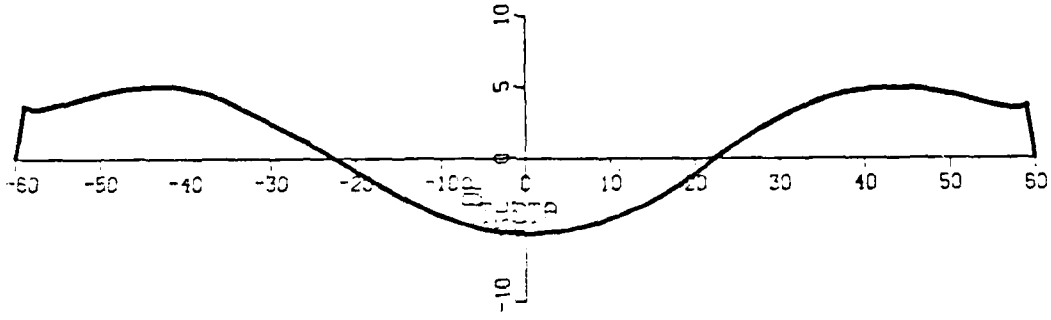

Nonporous Camber

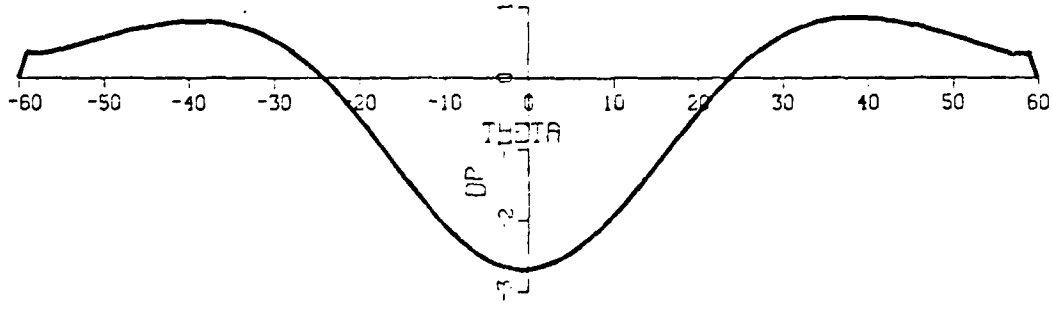

Porous Camber, $\alpha = 0.25$

Figure 19. **Differential Pressure Comparison at T = 14.52**

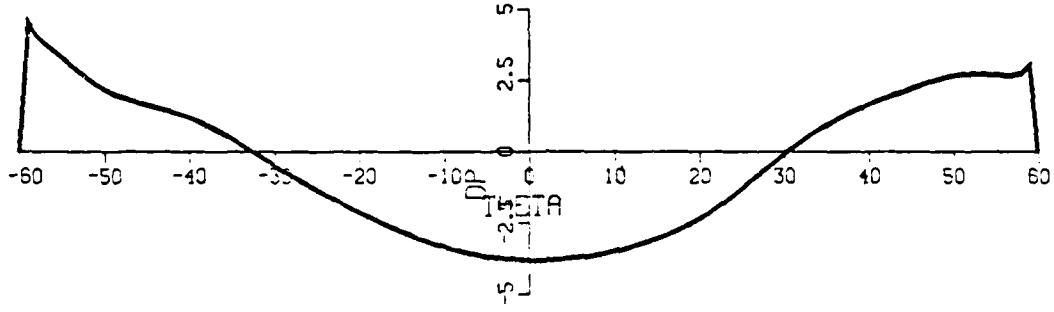

Nonporous Camber

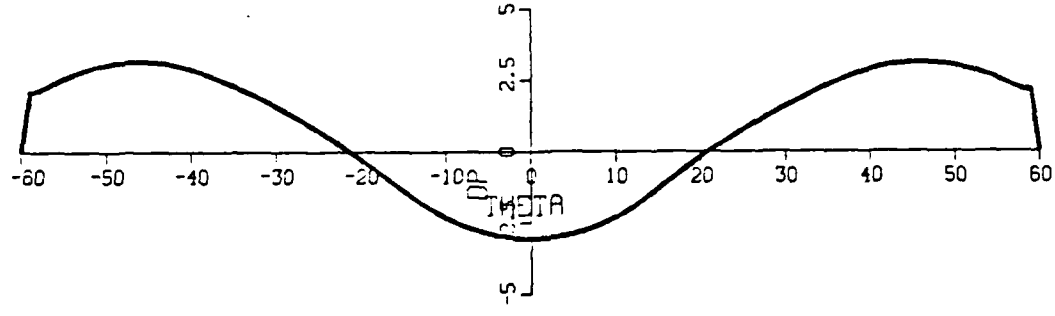

Porous Camber, $\alpha = 0.25$

Figure 20. **Differential Pressure Comparison at T = 16.98**

noted earlier, Inoue's method does not take into account the relationship between the flow and the differential pressure, or the variability of α along the camber and with time. In other words, α must vary with time and with the angle along the camber. Thus, the comparison of the $\alpha = 0.0$ and $\alpha = 0.25$ cases will not be made in greater detail than Inoue's method deserves.

C. PRESENT METHOD OF POROSITY MODELING

With the realization of the fact that the flow through the camber must be related to the prevailing differential pressure and that the direction of the flow in the wake has no measurable effect on the differential pressure versus dynamic head, a new method had to be devised which will properly account for the effect of porosity.

The present method takes advantage of the simplicity of Inoue's method and accounts for the local dependence of the flow on differential pressure. For this purpose, the value of α is chosen so as to make the V_N at $\theta = 0.0$ proportional to the $\sqrt{\Delta p}$ as given by Figure 4. The variations in the flow across the camber beyond and above that given by Inoue's method are accounted for through the use of discrete vortices placed along the camber. A number of sample calculations have shown that the use of 118 body vortices (one every degree) on a 120-degree camber will be more than sufficient to account for the additional cross-flow effects smoothly. The first vortices were placed one degree from the tips, and no vortex was placed at $\theta = 0$. The mid-points between the vortices were used as the control points to

calculate the velocity normal to the camber. At each control point, the differential pressure was calculated, and then V_N was found from

$$V_N = \frac{1}{C_p}\sqrt{\frac{2\Delta p}{\rho}}$$

The velocity induced by the uniform flow based on α was subtracted, and then the strengths of the body vortices were determined by equating the remaining velocity to that induced by the body vortices at the control points. Once the strengths of the body vortices were determined, the velocity induced at each vortex in the wake was calculated, the velocity of the ambient flow was updated, and all of the wake vortices were convected for a time interval Δt using a 2^{nd} order modified Eulerian scheme. Then the procedure was repeated, up to any specific time (in this analysis T = 24). The wake vortices were never merged together, no matter how close they came, and were only removed from the simulation if they contacted the camber. To prevent abnormally high induced velocities from occurring due to the proximity of one vortex to another, whether body or wake vortices, Rosenhead's (1930) smoothing scheme was used, where the complex velocity at a point was multiplied by

$$\frac{x^2}{x^2 + \delta^2}$$

where x is the distance from the point to the vortex inducing the velocity and δ is the attenuation factor. In this analysis, δ was chosen to be 0.05.

The method described above is quite general and could be used to investigate the effect of the porosity of any canopy. Because it is deemed sufficient to understand the physics of the phenomenon, only two canopy characteristics were used in the numerical experiments. The first case corresponded to the characteristics of canopy sample A (C_p = 22.9, see Table 2), and the second to a canopy which is much more porous than any of the samples tested, with an assumed C_p = 4.45, which corresponded to an initial value of α = 0.25 at θ = 0 and T = .5.

Figures 21 through 25 show the evolution of the wake for C_p = 22.9 (sample A). Comparison of these figures with Figures 11 through 15 shows that the effect of porosity, however noticeable, is not large enough to show a significant downstream displacement of the wake vortices. The importance of this conclusion lies in the fact that the most porous parachute canopy used by the industry is not sufficiently porous to minimize the consequences of the wake return, i.e., the collapse of the parachute as evidenced by field experiments. Thus, it has been possible through a relatively idealized analysis to show the inadequacies of the materials used in the construction of large parachutes.

The next step in the analysis was to show the beneficial effects of porosity when it can be made sufficiently large. For this purpose, a value of C_p = 4.45 was chosen, for the reasons noted earlier. Figures 26 through 30 show the evolution of the wake and Figures 31 through

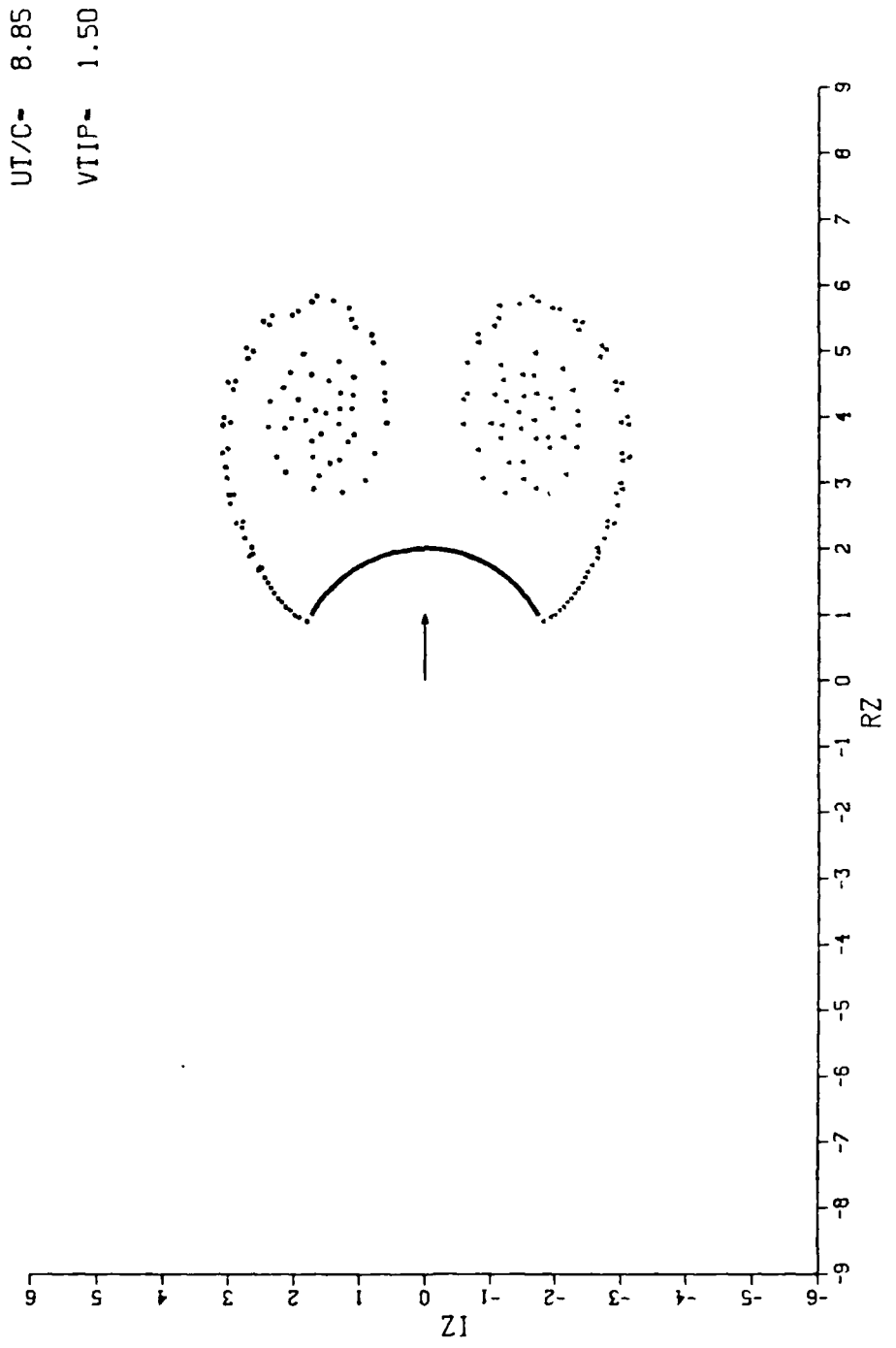

Figure 21. **Wake Vortex Positions for C_p = 22.9 at T = 8.85**

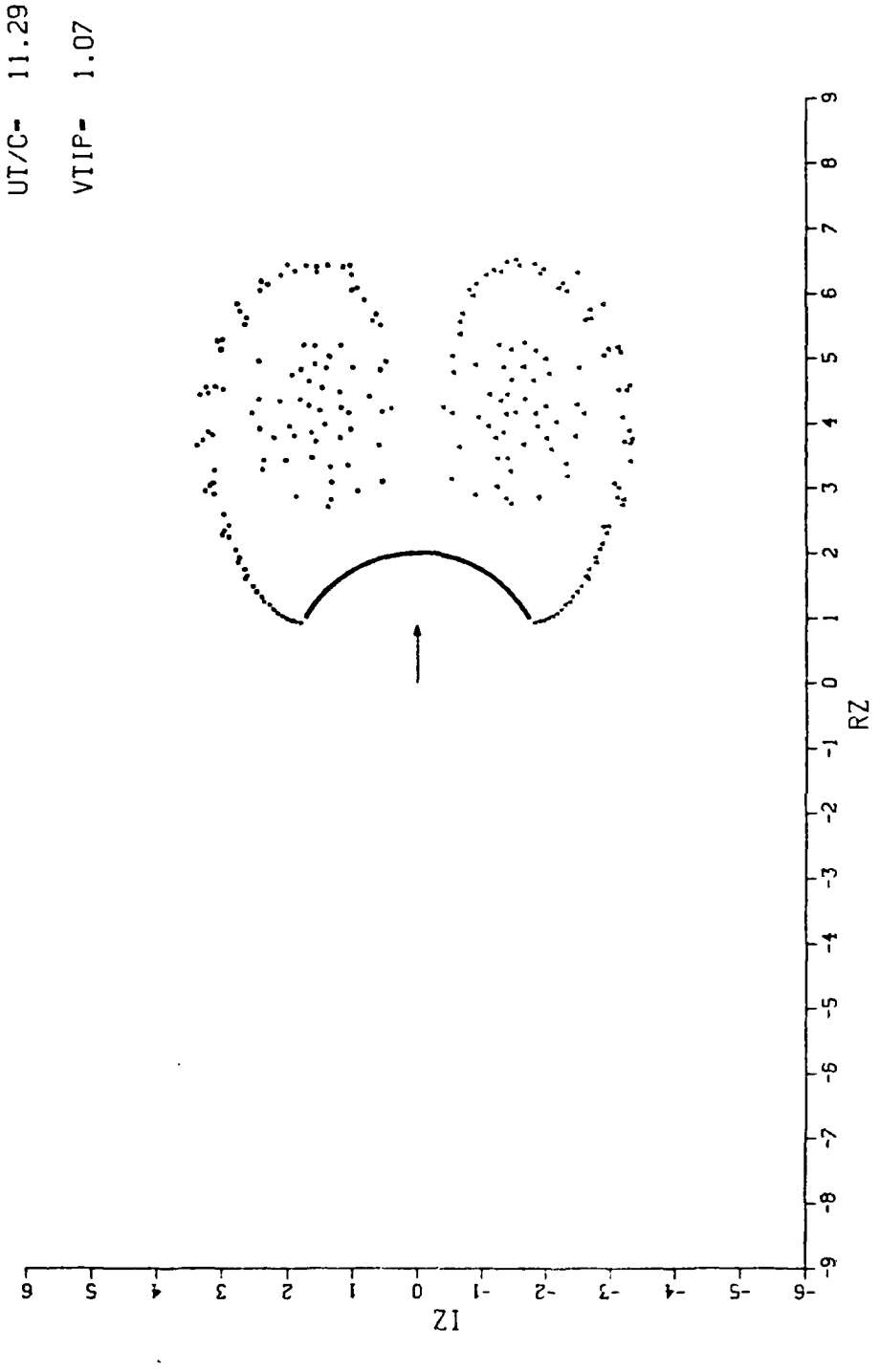

Figure 22. **Wake Vortex Positions for C_p = 22.9 at T = 11.29**

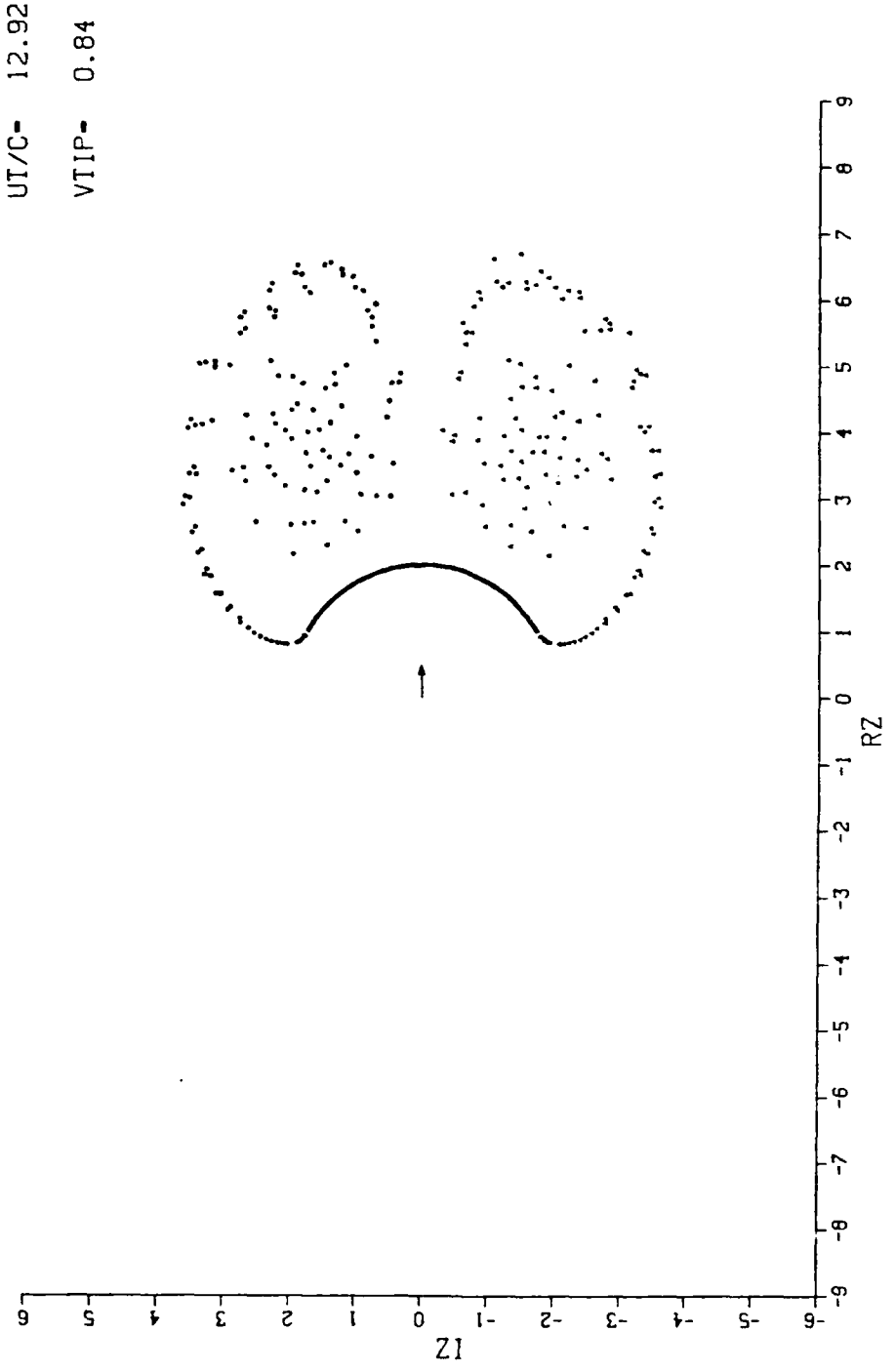

Figure 23. **Wake Vortex Positions for C_p = 22.9 at T = 12.92**

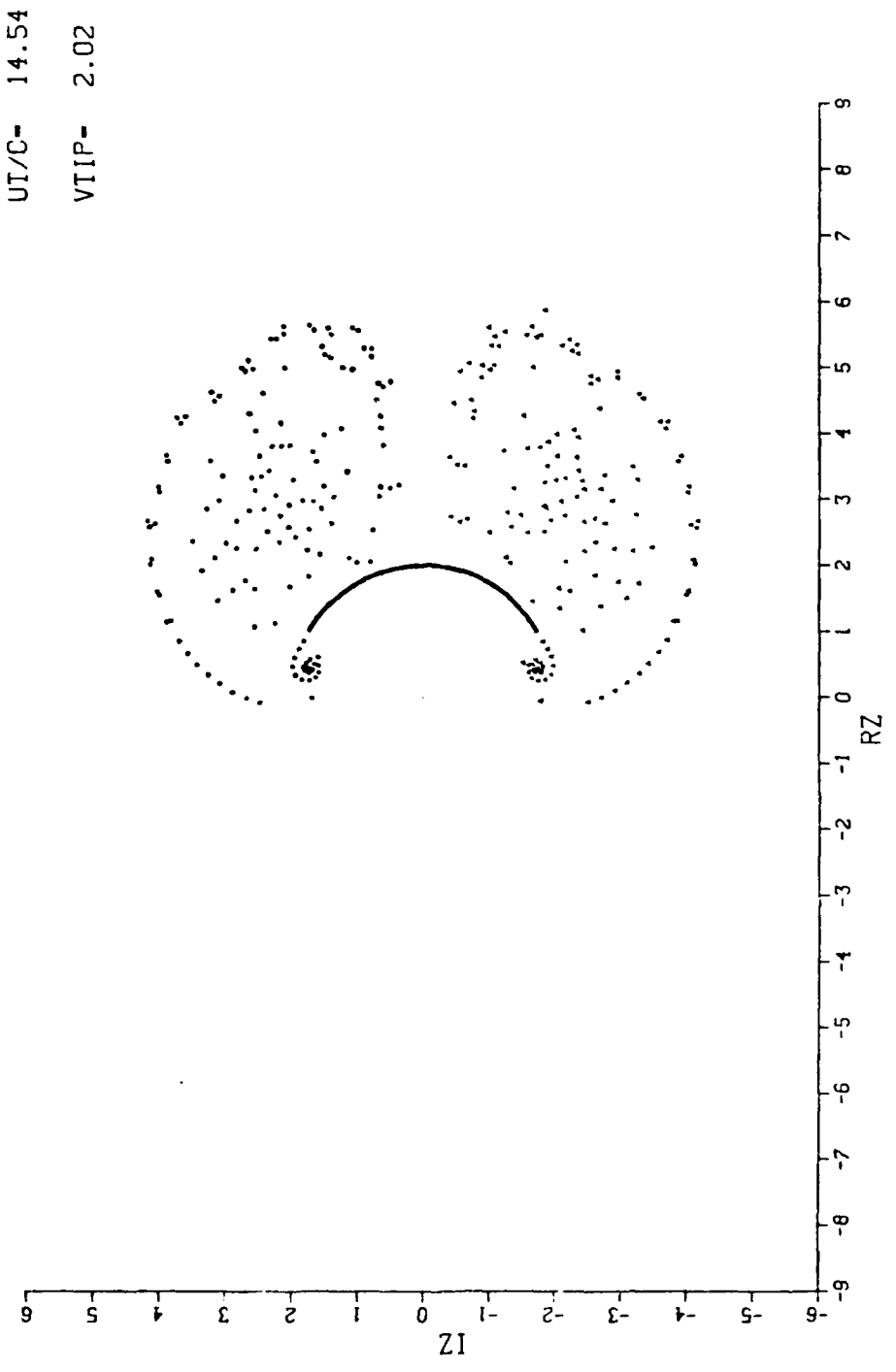

Figure 24. **Wake Vortex Positions for C_p = 22.9 at T = 14.54**

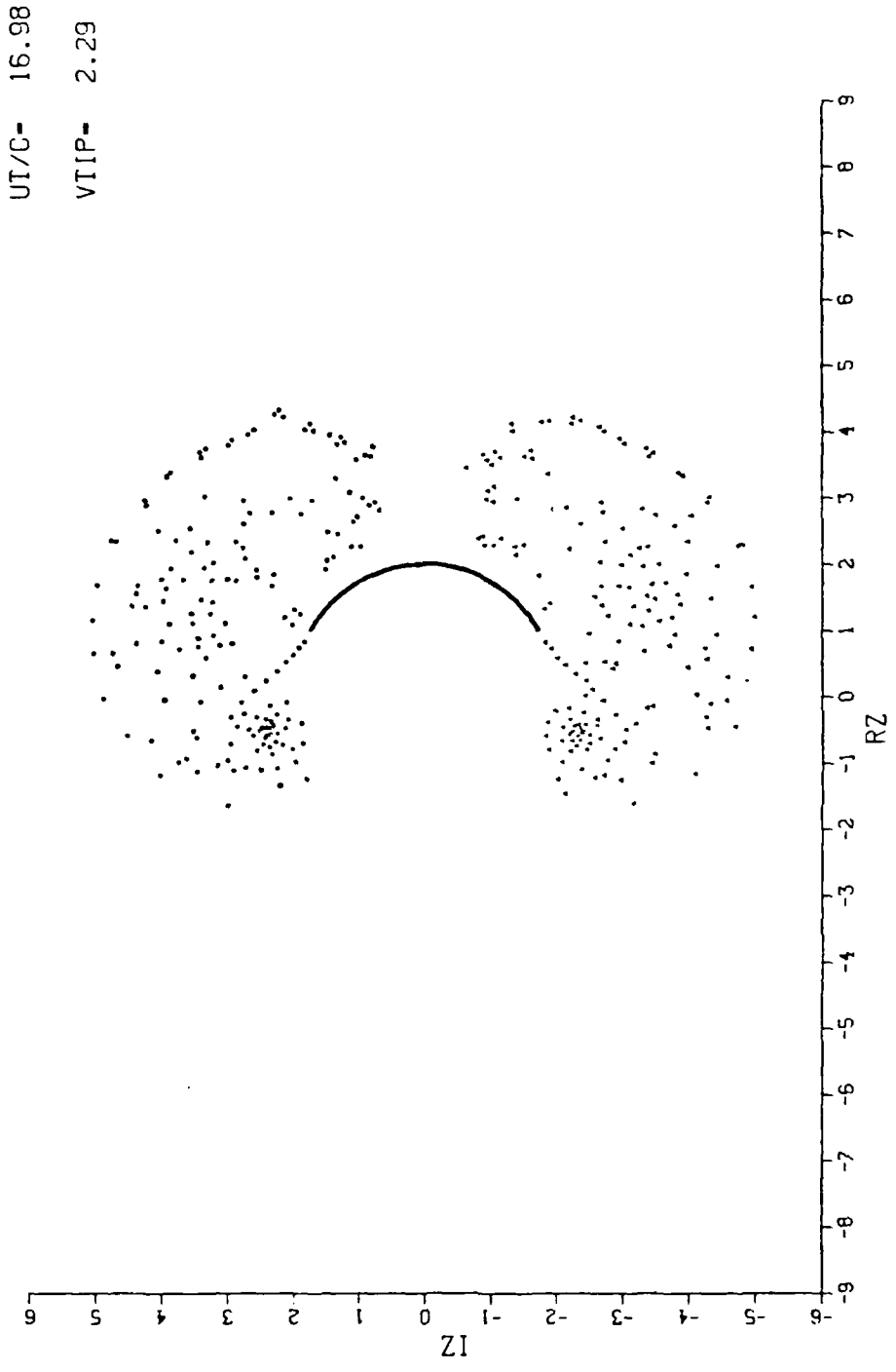

Figure 25. **Wake Vortex Positions for C_p = 22.9 at T = 16.98**

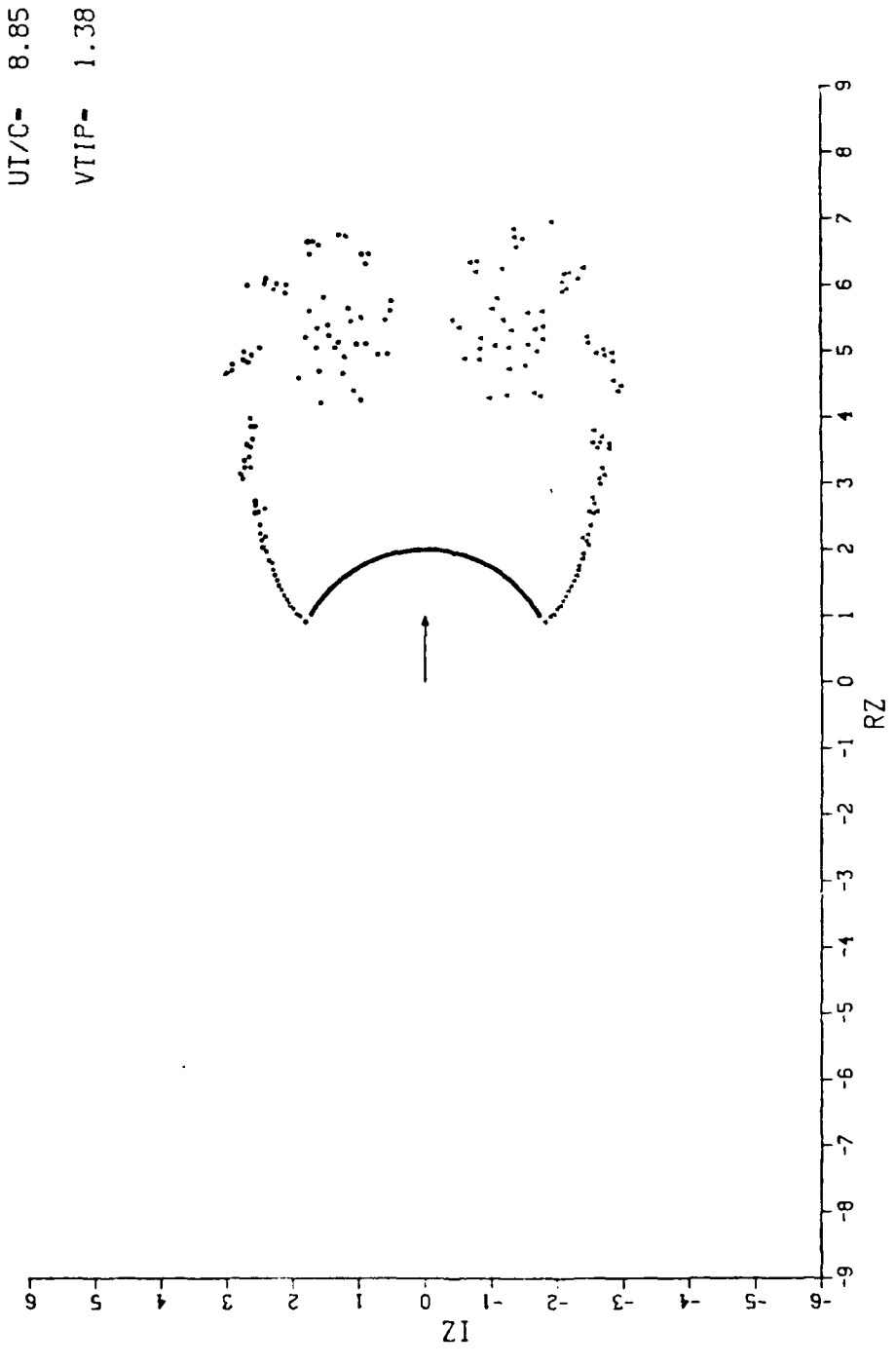

Figure 26. **Wake Vortex Positions for C_p = 4.45 at T = 8.85**

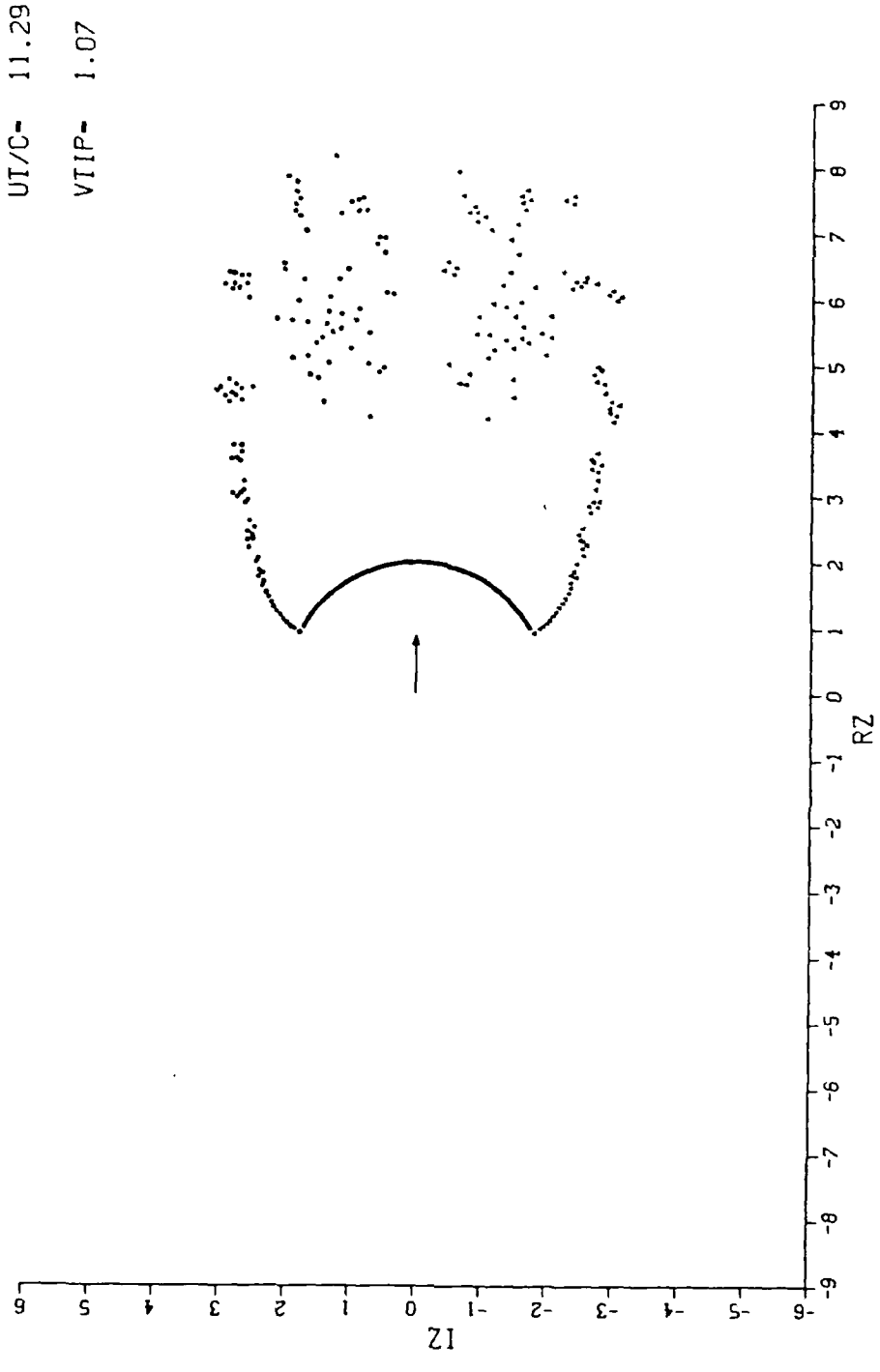

Figure 27. **Wake Vortex Positions for C_p = 4.45 at T = 11.29**

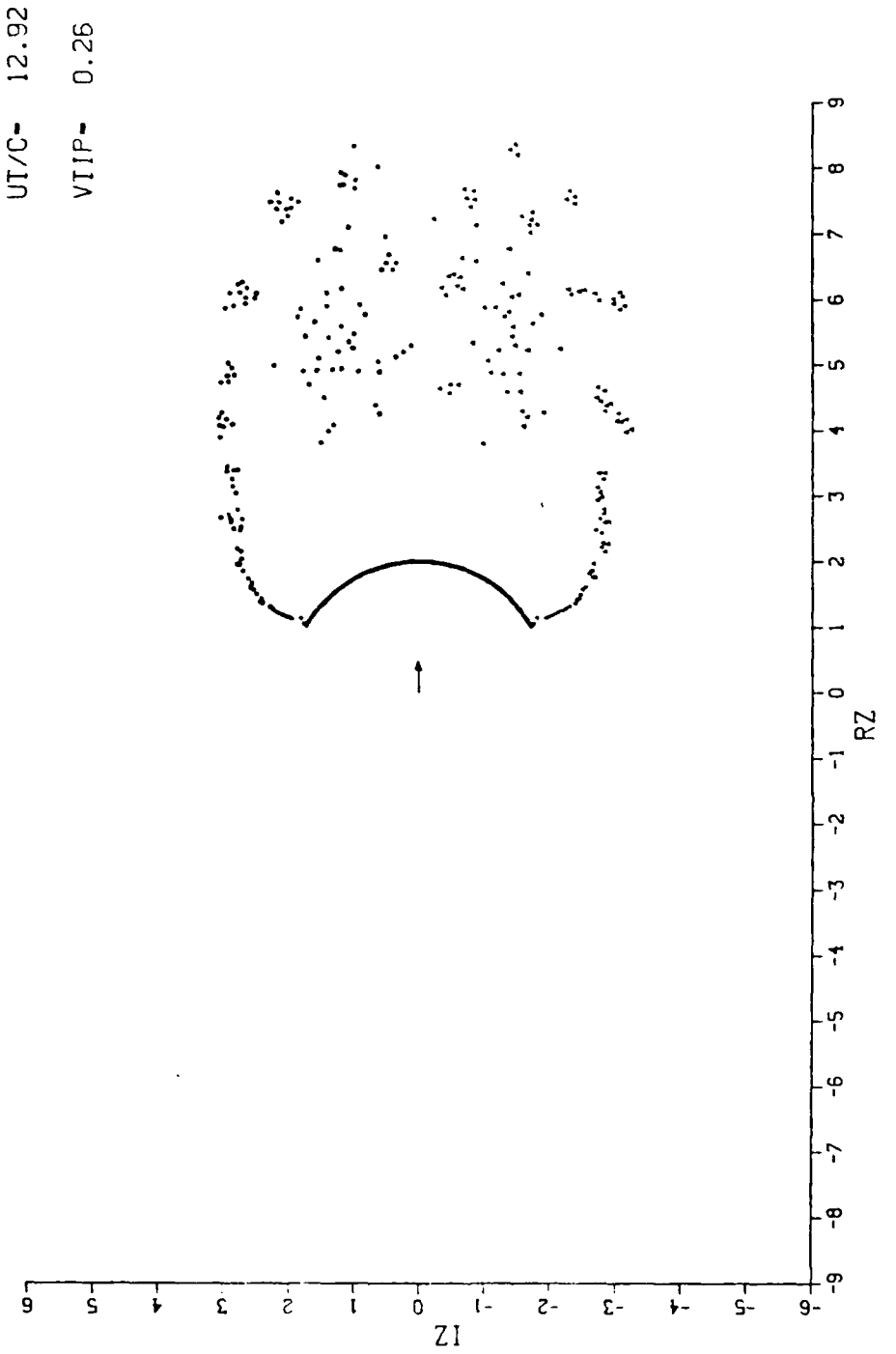

Figure 28. **Wake Vortex Positions for C_p = 4.45 at T = 12.92**

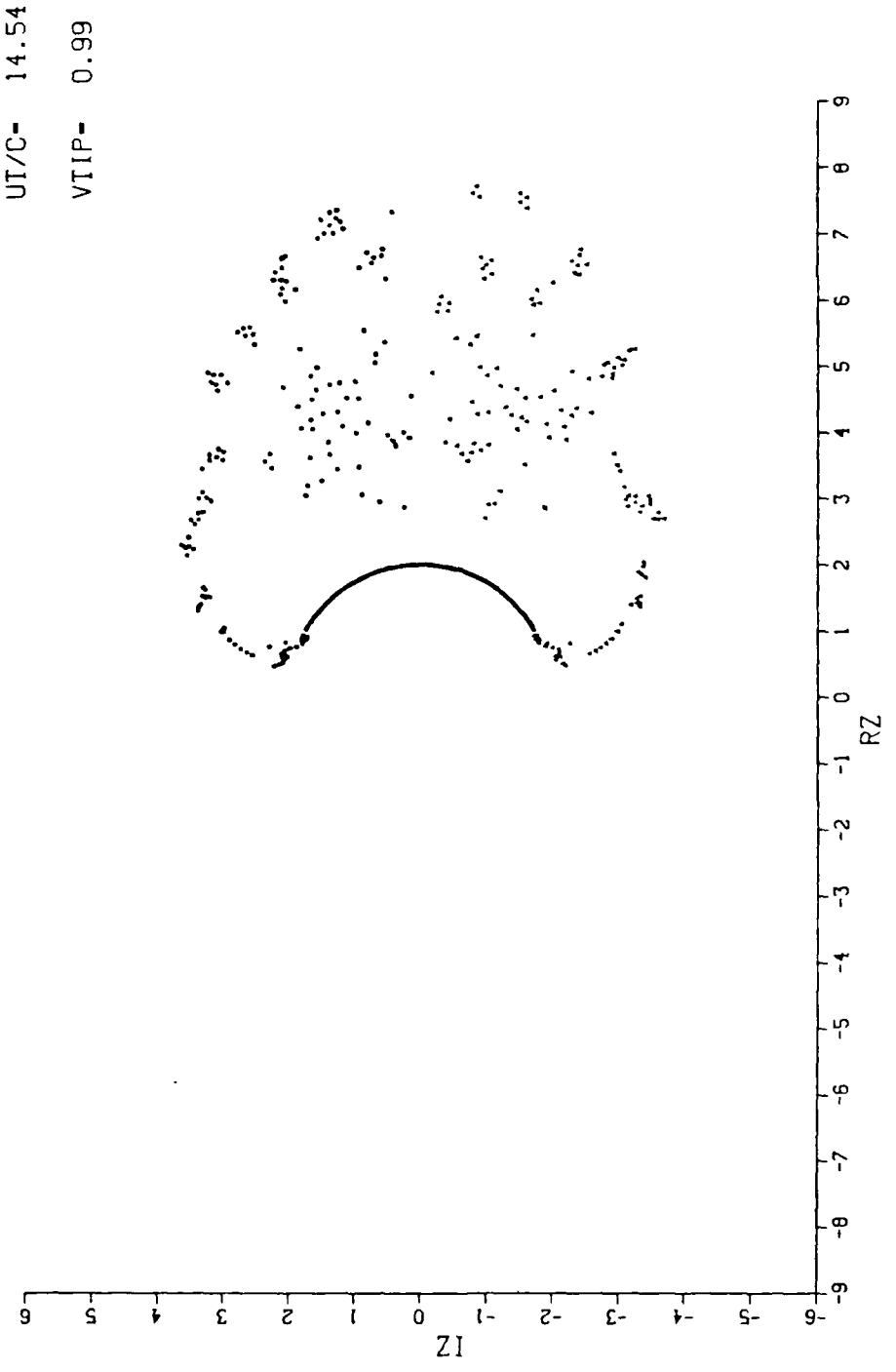

Figure 29. **Wake Vortex Positions for C_p = 4.45 at T = 14.54**

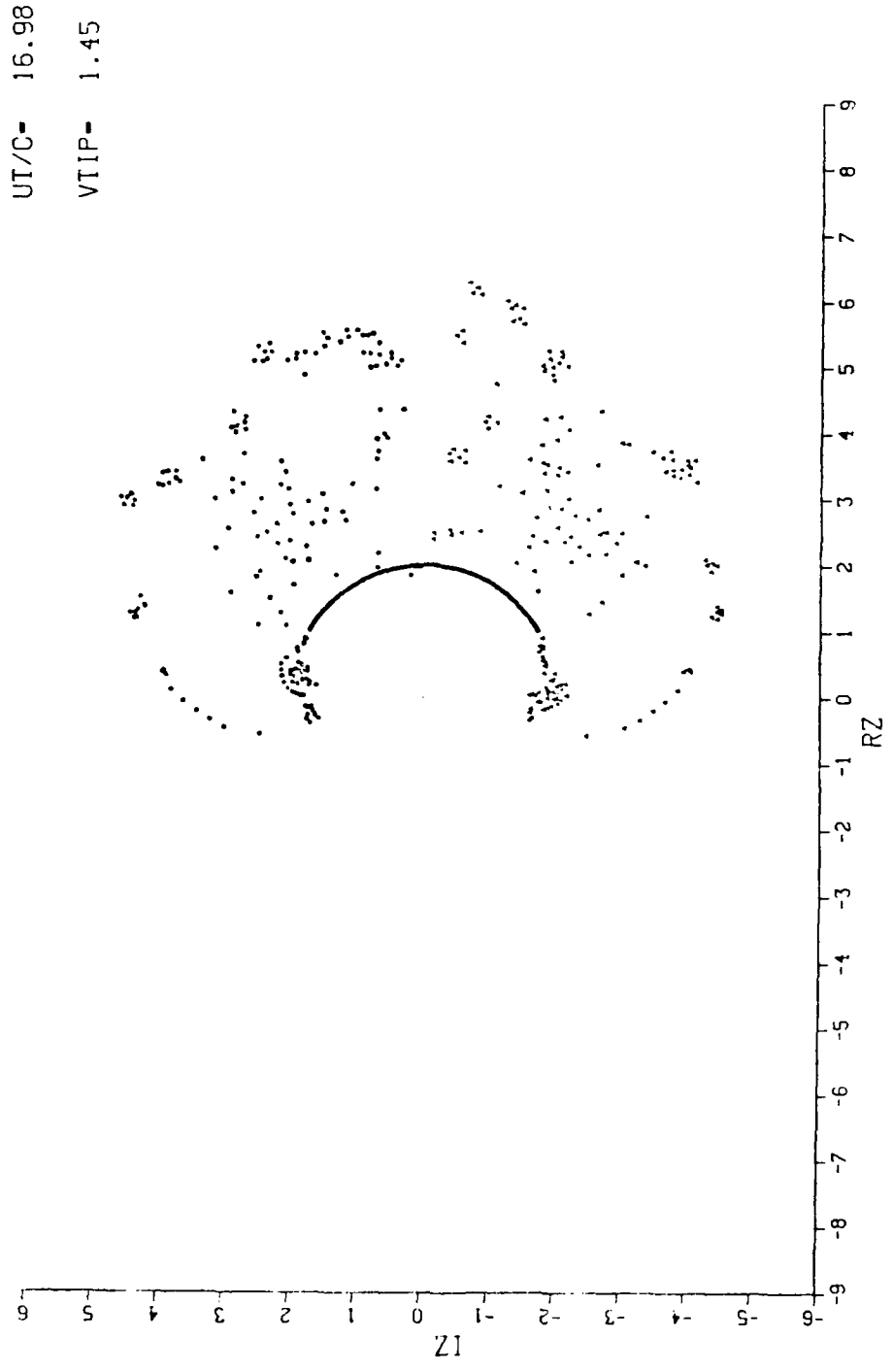

Figure 30. **Wake Vortex Positions for C_p = 4.45 at T = 16.98**

35 the differential pressures. It is evident from a comparison of Figures 26 through 30 with either Figures 11 through 15 (nonporous case) or Figure 21 through 25 (C_p = 22.9 case) that the wake is significantly displaced downstream and that, as seen in Figures 31 through 35, the differential pressure is far less negative than those shown in Figures 16 through 20 (α = .25 and α = 0.0). Figure 36 shows histories of the differential pressure computations at θ = 0 degrees for the nonporous case, the present model with C_p = 22.9, Inoue's method with α = 0.25, and the present model with C_p = 4.45. It is easily seen that the present method with C_p = 22.9 has differential pressures only slightly less in magnitude than the nonporous case, while the two other, more porous cases have differential pressures significantly smaller in magnitude and delay the occurrence of negative differential pressure at the center of the body. It is also seen that while the two large porosity cases during steady state and the early deceleration periods are very similar, during later stages of the deceleration the present method results in lower differential pressures as it accounts for the amount of flow through the body due to the local differential pressures.

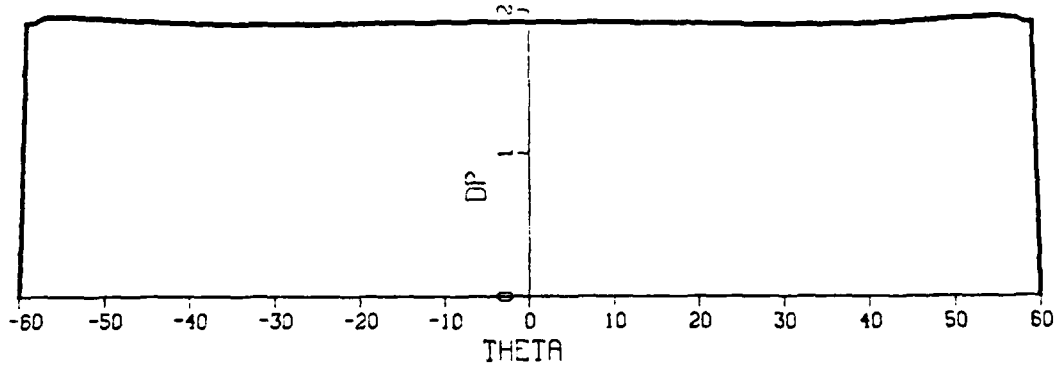

Figure 31. **Differential Pressure for C_p = 4.45 at T = 8.85**

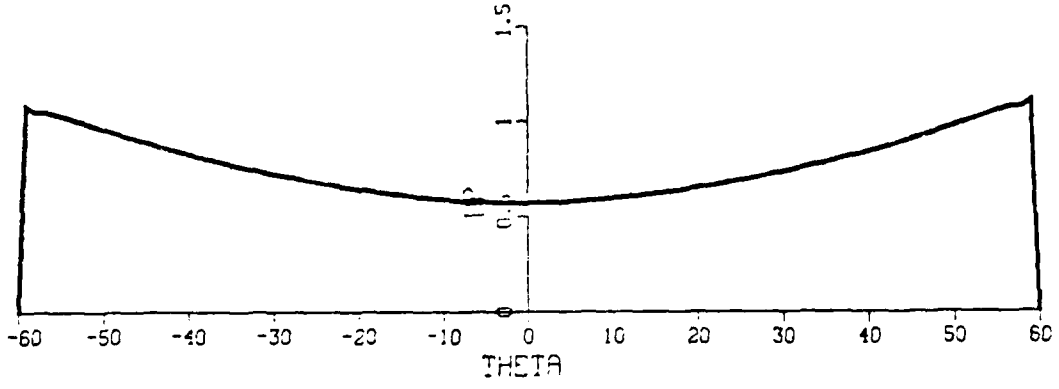

Figure 32. **Differential Pressure for C_p = 4.45 at T = 11.29**

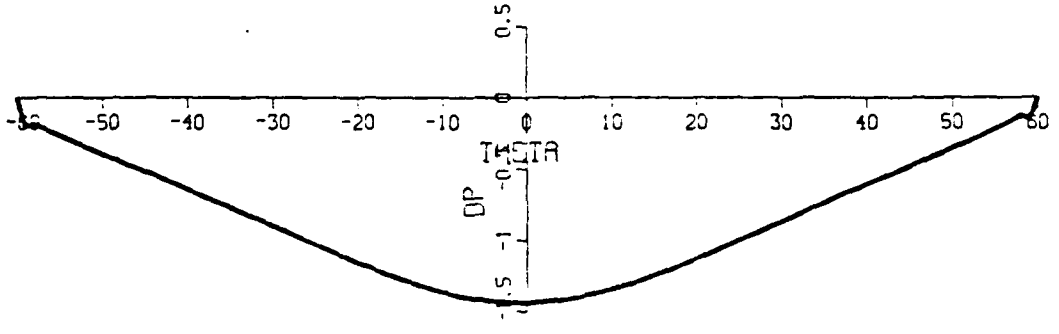

Figure 33. **Differential Pressure for C_p = 4.45 at T = 12.92**

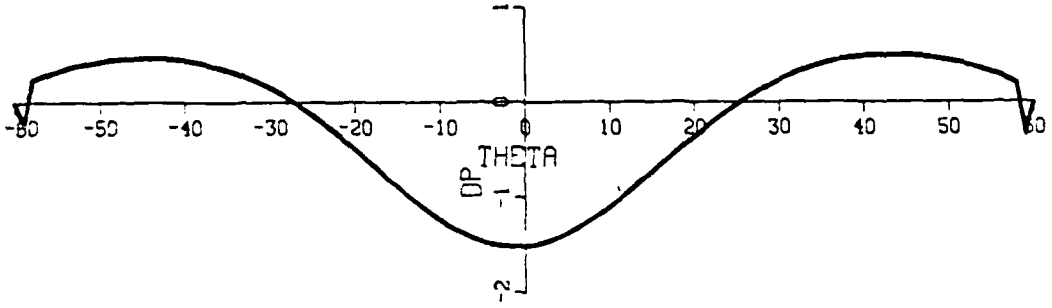

Figure 34. **Differential Pressure for C_p = 4.45 at T = 14.54**

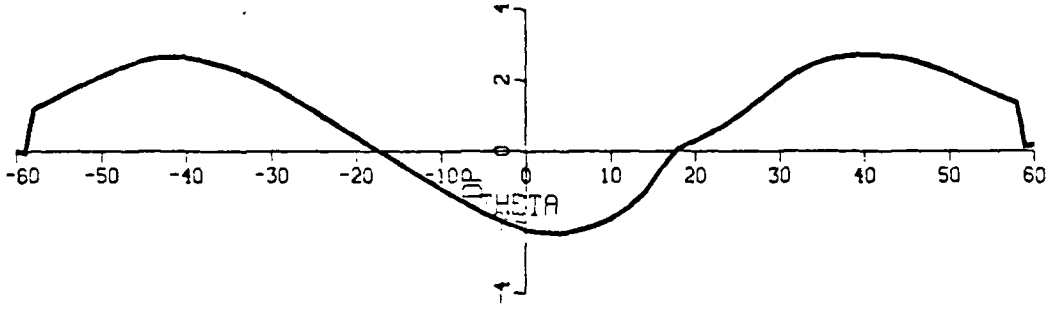

Figure 35. **Differential Pressure for C_p = 4.45 at T = 16.98**

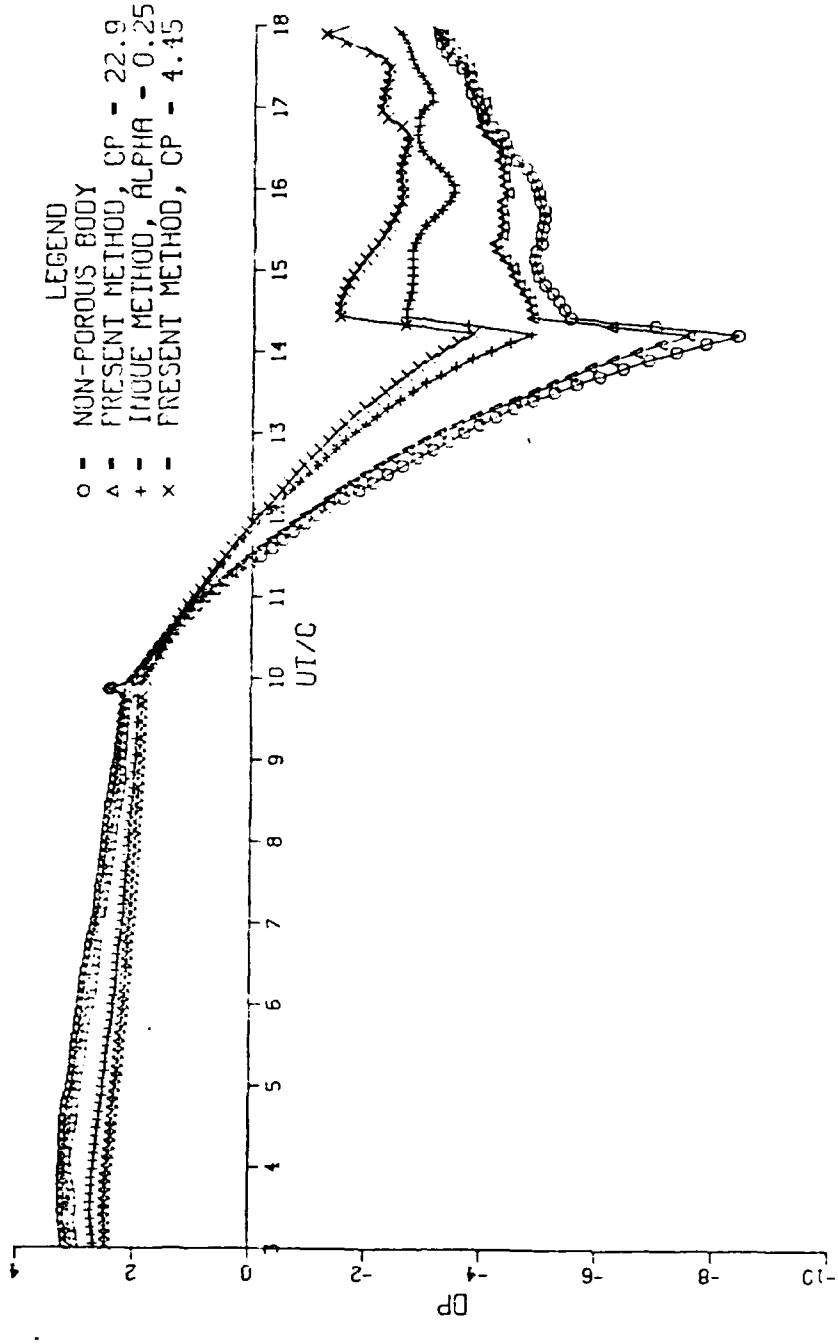

Figure 36. **Differential Pressure History Comparison**

IV. CONCLUSIONS

The results presented herein warranted the following conclusions.

1. The effect of porosity is a function of the differential pressure across the porous material, and is dictated only by the physical characteristics of the material.

2. For a given canopy, the normalized differential pressure (the pressure coefficient) is independent of the ambient velocity, up to a velocity of about 600 miles per hour.

3. The effect of porosity cannot be adequately accounted for by letting through the camber a constant uniform velocity, as done by Inoue. The effect of the variation of differential pressure with time and along the camber must be included.

4. A novel method has been devised which combines the uniform porous flow concept with the variability of the flow rate with differential pressure through the use of discrete vortices embedded in the camber.

5. The results have shown that, in general, the effect of porosity is to displace the wake vortices further downstream and to retard their return to the camber during the period of deceleration.

6. Even the most porous canopy material used in the construction of large parachutes is not sufficiently porous to prevent the collapse of the parachute, as evidenced by the field experiments and verified by the present numerical model.

7. The results of calculations with a much larger porosity have shown that it will be possible to considerably delay or entirely eliminate the collapse phenomenon. In doing so, it may be advantageous to optimize the radial distribution of porosity along the camber in order to achieve as large a drag force as possible. One must, however, bear in mind the fact that one also needs to account for the flexibility of the canopy. This forms the basis of the continuing efforts toward the understanding of the behavior of aerodynamic deceleration devices.

LIST OF REFERENCES

Baines, W. D., and Peterson, E. G. 1951, "An Investigation of Flow Through Screens," *Transactions of the ASME*, v. 73, pp. 467–480.

Chorin, A. J. 1973, "Numerical Study of Slightly Viscous Flow," *Journal of Fluid Mechanics*, v. 57, pp. 785–796.

Cumberbatch, E. 1982, "Two-Dimensional Flow Past a Mesh," *Quarterly Journal of Mechanics and Applied Mathematics*, v. 35, pt. 3, pp. 335–344.

Graham, J. M. R. 1976, "Turbulent Flow Past a Porous Plate," *Journal of Fluid Mechanics*, v. 73, pt. 3, pp. 565–591.

Inoue, O. 1985, "A New Approach to Flow Problems Past a Porous Plate," *AIAA Journal*, v. 23, no. 12, pp. 952–958.

Klimas, P. C., and Rogers, D. F. 1977, "Helium Bubble Survey of a Parachute-Opening Flowfield Using Computer Graphics Techniques," *Journal of Aircraft*, v. 14, no. 10, p. 952–958.

Koo, J.-K., and James, D. F. 1973, "Fluid Flow Around and Through a Screen," *Journal of Fluid Mechanics*, v. 60, pt. 3, pp. 513–538.

Laws, E. M., and Livesy, J. L. 1978, "Flow Through Screens," *Annual Review of Fluid Mechanics*, v. 10, pp. 247–266.

Mostafa, S. I. M. 1987, *Numerical Simulation of Unsteady Separated Flows*, Ph.D. Dissertation, Naval Postgraduate School, Monterey, California, June.

Munz, P. D. 1987, *Unsteady Flow About Cambered Plates*, M.S.M.E. Thesis, Naval Postgraduate School, Monterey, California, June.

Payne, P. R. 1978, "The Theory or Fabric Porosity as Applied to Parachutes in Incompressible Flow," *Aeronautical Quarterly*, v. 29, pt. 3, pp. 175–206.

Pepper, W. B., Jr. 1985, "A New Rotating Parachute Design Having High Performance," *Journal of Spacecraft*, v. 23, no. 2, pp. 222–224.

Reynolds, A. J. 1969, "Flow Deflection by Gauze Screens," *Journal of Mechanical Engineering Science*, v. 11, no. 3, pp. 290-294.

Rosenhead, L. 1930, "The Spread of Vorticity in the Wake Behind a Cylinder," *Proc. of the Royal Society*, v. 127, pp. 590-612.

Rychnovsky, R. E. 1977, "A Lifting Parachute for Very-Low-Altitude, Very-High-Speed Deliveries," *Journal of Aircraft*, v. 14, no. 2, pp. 184-187.

Sarpkaya, T. 1975, "An Inviscid Model of Two-Dimensional Vortex Shedding for Transient and Asymptotically Steady Separated Flow Over an Inclined Plate," *Journal of Fluid Mechanics*, v. 68, pp. 109-128.

Taylor, G. I. 1944, "Air Resistance of a Flat Plate of Very Porous Material," *Scientific Papers of Sir Geoffrey Ingram Taylor, G. K.*, F. R. S. Batchelor, ed., 1963, University Press, Cambridge, U.K., v. 3, pp. 383-386.

Taylor, G. I., and Davies, R. M. 1944, "The Aerodynamics of Porous Sheets," *Scientific Papers of Sir Geoffrey Ingram Taylor, G. K.*, F. R. S. Batchelor, ed., 1963, University Press, Cambridge, U.K., v. 3, pp. 391-405.

Turner, J. T. 1969, "A Computational Method for the Flow Through Non-Uniform Gauzes: The General Two-Dimensional Case," *Fluid Mechanics*, v. 36, pt. 2, pp. 367-383.

Wieghardt, K. E. G. 1953, "On the Resistance of Screens," *Aeronautical Quarterly*, v. 4, pp. 186-192.

INITIAL DISTRIBUTION LIST

		No. Copies
1.	Defense Technical Information Center Cameron Station Alexandria, VA 22304-6145	2
2.	Library, Code 0142 Naval Postgraduate School Monterey, CA 93943-5002	2
3.	Department Chairman, Code 69 Naval Postgraduate School Monterey, CA 93943-5000	2
4.	Prof. T. Sarpkaya, Code 69SL Naval Postgraduate School Monterey, CA 93943-5000	6
5.	Mr. Louis G. Lindsey 125 Alton Avenue San Francisco, CA 94116	1
6.	Mr. John J. Andrews 8180 Santa Arminta San Diego, CA 92126	1
7.	Commander David W. Taylor Naval Ship Research and Development Center Bethesda, MD 20084	2
8.	Commander Naval Weapons Center China Lake, CA 93555	2
9.	LT Paul J. Lindsey 125 Alton Avenue San Francisco, CA 94116	5